Exposure to 3, 3', 4, 4', 5-pentachlorobiphenyl (PCB 126) causes widespread DNA hypomethylation in adult zebrafish testis

Neelakanteswar Aluru[1] and Jan Engelhardt[2,3]

[1]Biology Department and Woods Hole Center for Oceans and Human Health, Woods Hole Oceanographic Institution, Woods Hole, MA 02543

[2]Bioinformatics Group, Department of Computer Science and Interdisciplinary Center for Bioinformatics, University of Leipzig, Härtelstraße 16-18, D-04107, Leipzig, Germany

[3]Department of Evolutionary Biology, University of Vienna, Djerassiplatz 1, A-1030 Vienna, Austria

Key words: DNA methylation, zebrafish, dioxin-like PCBs, testis, environmental epigenetics

Short title: *PCB126 induced epigenetic changes in zebrafish testis*

Abstract

Exposure to environmental toxicants during preconception have been shown to affect offspring health and epigenetic mechanisms such as DNA methylation are hypothesized to be involved in adverse outcomes. However, studies addressing the effects of exposure to environmental toxicants during preconception on epigenetic changes in gametes are limited. The objective of this study is to determine the effect of preconceptional exposure to a dioxin-like PCB (PCB126) on DNA methylation and gene expression in testis. Adult zebrafish were exposed to 3 and 10 nM PCB126 for 24 hours and testis tissue was sampled at 7 days post-exposure for histology, DNA methylation and gene expression profiling. Reduced Representation Bisulfite Sequencing revealed 37 and 92 differentially methylated regions (DMRs) in response to 3 and 10nM PCB126 exposures, respectively. Among them 19 DMRs were found to be common between both PCB126 treatment groups. Gene ontology (GO) analysis of DMRs revealed that enrichment of terms such as RNA processing, iron-sulfur cluster assembly and gluconeogenesis. Gene expression profiling showed differential expression of 40 and 1621 genes in response to 3 and 10nM PCB126 exposures, respectively. GO analysis revealed differential expression of genes related to xenobiotic metabolism, oxidative stress and immune function. There is no overlap in the GO terms or individual genes between DNA methylation and RNAseq results, but functionally many of the altered pathways have been shown to cause spermatogenic defects.

Impact statement: Our results indicate that exposure to dioxin-like PCBs during preconception could affect testicular function by altering DNA methylation patterns, with significant implications for reproductive health.

Introduction

Polychlorinated biphenyls (PCBs) are one of the most persistent and widespread group of endocrine disrupting compounds in our environment. Although PCBs are no longer produced, they remain a toxic legacy to the environment and to human health (Faroon and Ruiz 2016). The most toxic PCBs are non-ortho substituted congeners (dioxin-like PCBs) such as 3, 3', 4, 4', 5-pentachlorobiphenyl (PCB126) (Safe 1990). Both epidemiological and experimental studies have demonstrated adverse effects of exposure to PCBs ranging from developmental defects to reproductive abnormalities (Coulter et al. 2019; Khanjani and Sim 2007; Meeker and Hauser 2010). The reproductive abnormalities include disruption of endometrial physiology in females and disruption of spermatogenesis in males. Decrease in sperm count is one of the most sensitive indicators of dioxin and dioxin-like PCBs toxicity and spermatogenesis is considered a window of susceptibility (Mocarelli et al. 2011). Several studies have demonstrated the impacts of toxicant exposure during pre-conception on germ cell development as well effects on the next generation (Day et al. 2016; Venkatratnam et al. 2021; Viluksela and Pohjanvirta 2019; Zhang et al. 2020).

As epigenetic reprogramming occurs during spermatogenesis, there have been several studies investigating the relationship between aberrant germ line epigenetic modifications (DNA methylation and chromatin state) and testicular function. Epidemiological studies have determined an association between dioxin-like PCBs and global DNA methylation in humans (Kim et al. 2010; Lind et al. 2013; Pittman et al. 2020; Ruiz-Hernandez et al. 2015; Rusiecki et al. 2008). Among elderly Swedish population, high levels of PCB126 are associated with DNA hypermethylation (Lind et al., 2013). In young Icelandic Inuit and Korean populations persistent organic pollutant exposure including dioxin-like PCBs is correlated with DNA hypomethylation (Kim et al., 2010; Rusiecki et al., 2008). These contradictory findings could be due to age of the

study participants, presence of a mixture of POPs in human serum samples and the methods used for quantifying global DNA methylation. Even though global DNA methylation quantification methods provide useful information, they quantify methylation changes of transposable elements such as LINE-1 or Alu repeats (Yang et al. 2004) or quantify total number of methylated cytosines in DNA (Tellez-Plaza et al. 2014). Both these methods do not provide functionally relevant information. In contrast, recent epidemiological and experimental animal studies investigating transgenerational effects of exposure have used genomewide approaches such as CpG arrays, MeDIP, RRBS or WGBS to quantify DNA methylation changes (Akemann et al. 2020; Aluru et al. 2018; Manikkam et al. 2012; Pittman et al., 2020). Using bioinformatics these changes have been associated with genes.

For instance, gestational exposure to dioxin (TCDD) has been shown cause transgenerational effects in mice (Manikkam et al., 2012). Even though this study did not observe any phenotypic changes in the testis in either the exposed or subsequent generations, they observed DNA methylation changes in the F3 generation sperm epigenome. Similarly, developmental exposure to TCDD has been shown to cause male specific reproductive defects in F1 and F2 generations in zebrafish and these changes have been associated the phenotypes to testicular DNA methylation changes (Akemann et al., 2020). These studies have established the potential long-term effects of early life exposure to dioxin. However, very little is known about the effects of exposure environmental chemicals during preconception, a susceptible window of germ cell development (Heindel 2019). There is a growing consensus that preconception exposure to environmental toxicants can adversely affect not only reproductive outcomes such as fertility and pregnancy but also affect fetal development (Segal and Giudice 2019). Yet, the mechanisms by which environmental chemicals disrupt germ cell development and function are not well understood.

The objective of this study is to characterize the effects of exposure to a dioxin-like PCB (PCB126; 3,3',4,4',5-pentachlorobiphenyl) on testis morphology and genome-wide changes in DNA methylation and gene expression patterns. We used PCB126 as a model compound as it is still present in the environment and in human blood samples (Xue et al. 2014). In addition, PCBs (including PCB126) are categorized as group 1 human carcinogen by the International Agency for Research on Cancer, an intergovernmental agency of the World Health Organization (Lauby-Secretan et al. 2016). Furthermore, PCB126 is a well-established agonist of aryl hydrocarbon receptor (AHR), a ligand-activated transcription factor and a member of the basic-region-helix-loop-helix PER/ARNT/SIM (bHLH-PAS) superfamily of transcription factors (Avilla et al. 2020). AHR activation regulates various signaling pathways including development, detoxification, immune response, energy metabolism, nervous system and reproduction. We exposed adult zebrafish to two different concentrations (3 and 10nM) of PCB126 for 24 hours via water borne exposure and raised them in contaminant free water for 7 days before sampling testis for histological, transcriptomic and DNA methylation profiling. We have previously demonstrated that this exposure regime alters DNA methylation patterns in the liver and brain tissues (Aluru et al., 2018).

Materials and Methods

Experimental Animals

The animal husbandry and experimental procedures used in this study were approved by the Animal Care and Use Committee of the Woods Hole Oceanographic Institution. Adult Tupfel/Long fin mutations (TL) strain of zebrafish were used in this study. Fish were maintained in 10 L tanks (density of 2 fish per liter) at 28±0.5°C system water with a 14-h light, 10-h dark cycle. The fish were fed twice daily; morning feeding with freshly hatched brine shrimp (*Artemia salina*) and afternoon feeding with GEMMA Micro 300 microencapsulated diet (Skretting USA, Tooele, Utah).

PCB126 Exposure

Adult male zebrafish (6 months old) were exposed to either 3 or 10 nM PCB126 or solvent carrier (0.01% DMSO) in system water (475 mg/l Instant Ocean, 79 mg/l sodium bicarbonate and 53 mg/l calcium sulfate; pH 7.2) for 24 h. We chose a 24 h exposure period based on our previous study where similar route of exposure resulted in AHR activation (Aluru et al., 2018). Exposures were carried out in 2 gallon capacity glass aquarium tanks in 5 L of water at density of 1 fish per 1.25 L of water.

Each treatment had either 5 or 6 biological replicates. At the end of the exposure, fish were transferred to clean water with constant aeration and heating and maintained for 7 days. Fish were not fed during the 24 h exposure period. During the 7 days post-exposure, the husbandry conditions were the same as described in the previous section. At 7 days post-exposure, fish were euthanized with MS-222 (150 mg/l) buffered with sodium bicarbonate (pH 7.2) prior to tissue sampling. We chose this experimental design in order to capture both primary and secondary changes in DNA methylation and gene expression. Testis were dissected out and a sub-sample was stored in 4% paraformaldehyde. Remaining sample of testis was snap frozen in liquid nitrogen and stored at –80°C until nucleic acids were isolated.

Histological analysis

Testis tissue samples were fixed in 4% paraformaldehyde (PFA) for at least 24 hours followed by dehydration through a series of graded ethanol solutions. Paraffin embedding and hematoxylin and eosin (H&E) staining were done following established protocols by Mass Histology services (Worcester, Massachusetts). Histology was done on testis from 6 animals per treatment group and 5-6 slides were analyzed for each fish. Images were taken using 63x objective on a Zeiss Airy Scan LSM800 confocal microscope.

Isolation of Total RNA and Genomic DNA

Simultaneous isolation of genomic DNA and total RNA was performed using the ZR-Duet™ DNA/RNA Mini Prep kit (Zymo Research, CA). RNA was treated with DNase during the isolation process. DNA and RNA were quantified using the Nanodrop Spectrophotometer. The quality of DNA and RNA was checked using the Agilent 4200 and 2200 Tape Station systems, respectively. The DNA and RNA integrity numbers of all samples were between 9 and 10.

Quantitative Real-Time PCR

Complementary DNA was synthesized from 0.5 µg total RNA using the iScript cDNA Synthesis Kit (Bio-Rad, CA). Quantitative PCR was performed with iQ SYBR Green Supermix in a MyiQ Single-Color Real-Time PCR Detection System (Bio-Rad, CA). Real-time PCR primers used for amplifying β-actin were 5'-CAACAGAGAGAAGATGACACAGATCA-3' (Forward) and 5'-GTCACACCATCACCAGAGTCCATCAC-3' (Reverse). These primers amplify both β-actin paralogs (*actb1* and *actb2*). C*yp1a* forward and reverse primers were 5'-GCATTACGATACGTTCGATAAGGAC-3' and 5'-GCTCCGAATAGGTCATTGACGAT-3', respectively. Both these primer sets span exon-intron boundaries to avoid any genomic DNA amplification. These primers have been previously used to quantify *cyp1a* expression (Aluru et al., 2018).

The PCR conditions used were 95°C for 3 min (1 cycle) and 95°C for 15 s/65°C for 1 min (40 cycles). At the end of each PCR run, a melt curve analysis was performed to ensure that only a single product was amplified. Three technical replicates were used for each sample. A no-template control was included on each plate to ensure the absence of background contamination. We did not observe any significant differences in β-actin levels between DMSO and PCB126 both in qPCR and in our RNAseq data. Relative expression was normalized to that of β-actin ($2^{-\Delta Ct}$; where $\Delta Ct = [Ct(cyp1a) - Ct(\beta\text{-}actin)]$). One-way ANOVA was used to determine

the effect of PCB126 on *cyp1a* induction (GraphPad Prism version 5.3). A probability level of $P < 0.05$ was considered statistically significant.

Reduced Representation Bisulfite Sequencing (RRBS) and Data Analysis

RRBS library preparation and sequencing was conducted by NXT-Dx, a Diagenode company (Ghent, Belgium). Briefly, libraries were prepared from 500 ng of genomic DNA digested with 30 units of MspI (New England Biolabs, MA), followed by end repair and A-tailing of DNA fragments. Fragments were ligated with methylated Illumina adapters. Adaptor-ligated fragments were size selected and then bisulfite converted using a commercial kit. Ligated fragments were amplified and the resulting products were purified and 50 bp paired end sequencing was performed on an Illumina HiSeq2500 platform. Sequence reads from RRBS libraries were identified using standard Illumina base-calling software (Cassava v.1.8.2).

Raw reads were pre-processed using TrimGalore (v0.4.3) and cutadapt (v1.12). FASTQC (v.0.10.1) was used to determine the quality of the sequencing reads. Pre-processed reads were aligned to the zebrafish genome (GRCz10) using the Bisulfite Analysis Toolkit (BAT; (Kretzmer et al. 2017)). BAT is an integrated toolkit that includes aligning the reads to the genome, calling differentially methylated regions (DMRs) using metilene (Juhling et al. 2016), annotation of DMRs, statistical analysis and correlating DMRs with gene expression. This is in contrast to prevalent methods where separate pipelines are used for mapping, DMR calling and statistical analysis. A comparison of different DNA methylation profiling pipelines to identify DMRs using RRBS data demonstrated that in most cases metilene has the highest precision (Liu et al. 2020).

After the read mapping the sequencing runs, one control (D1) and one 3nM PCB126 group (P3-12) were considered as outliers and were excluded from the subsequent analysis. Only cytosine

positions in a CpG context with at least 10 and at most 100 overlapping reads were considered. The DMRs were required to contain at least 10 of such cytosines. The minimum difference of mean methylation rates per group was at least 0.1 and only DMRs with an adjusted p-value of 0.05 were considered significant. The adjusted p-values were calculated using a Mann-Whitney U test with Bonferroni correction (Juhling et al., 2016). We classified the DMRs into various genic (promoters, introns and exons) and intergenic regions, CpG island and shores and repetitive elements using UCSC table browser.

DMR Gene Ontology Enrichment Analysis

We used Genomic Regions Enrichment of Annotations Tool (GREAT) to associate DMRs with genes (McLean et al. 2010). GREAT predicts gene functions of cis regulatory elements by assigning each gene a regulatory domain. To use GREAT, we converted the genomic coordinates of DMRs from GRCz10 version to Zv9 version of the genome using the UCSC genome browser liftOver utility (https://genome.ucsc.edu/cgi-bin/hgLiftOver). We used default parameters with a basal domain that extends 5 kb upstream and 1 kb downstream of the transcriptional start site and conducted gene ontology (GO) (biological process and molecular function) enrichment analysis.

RNA sequencing (RNAseq)

Stranded RNAseq library preparation using the Illumina TruSeq total RNA library prep kit and 50 bp single-ends sequencing on the HiSeq2000 platform were performed at the Tufts University Core Facility. Raw data files were assessed for quality using FastQC (Andrews 2010) and pre-processed as described previously. Data analysis was done as described previously (Aluru et al., 2018) by mapping the pre-processed reads to the Ensembl version 90 (GRCz10) of the zebrafish genome. Mapped reads were counted using HTSeq-count (Anders et al. 2015). Statistical analysis was conducted using DESeq2, a Bioconductor package (Love et

al. 2014). DESeq2 uses a Wald test with Benjamini and Hochberg correction. Only genes with false discovery rate (FDR;(Benjamini and Hochberg 1995) of less than 5% were considered to be differentially expressed.

Gene Ontology (GO) term enrichment analysis was performed using gProfiler package g:GOSt (Reimand et al. 2016). The up- and down-regulated differentially expressed genes (DEGs) from the high PCB126 group were analyzed separately. Ensembl Gene IDs of DEGs were used as input. The resulting output of significantly enriched GO Biological Process (BP) and Molecular Function (MF) terms were used as input in REVIGO (Supek et al. 2011) to remove redundant GO terms. The resulting GO terms were used to draw visualizations using CirGO (Kuznetsova et al. 2019). CirGO allows hierarchical visualization, where the inner circle represents the parent terms and the outer circle shows descendant child terms. Child terms are sorted based on statistical significance and highlighted with a color gradient.

Raw RRBS and RNAseq data have been deposited into Gene Expression Omnibus (Accession number GSE190741) and processed data has been deposited in Dryad (Aluru and Engelhardt 2022). In addition, the RRBS and RNAseq data can be visualized through the UCSC genome browser track hub: http://www.bioinf.uni-leipzig.de/~jane/Neel/testisRRBSHub/hub.txt. The instructions for visualizing the data are provided in the supplementary information.

Results

CYP1A expression in testis

We quantified *cyp1a* gene expression using quantitative real-time PCR, to confirm the activation of AHR by PCB126 (**Figure 1**). There was a concentration dependent increase in *cyp1a* expression. This result was confirmed by RNAseq with 190 and 480-fold induction in *cyp1a* expression in response to 3 and 10 nM PCB126 exposure.

Histology

There were no discernible histological changes in testis in response to PCB126 exposure (**Supplemental Figure 1**). Segmentation of different cell types using Image J did not show any significant differences in the number of spermatogonia, spermatocytes and spermatids between DMSO and PCB126 exposed groups (3 and 10 nM). The raw count data is provided in the supplemental information.

DNA methylation profiles in testis

Using eRRBS, we sequenced an average of 11.9 million paired-end reads per sample. The bisulfite conversion efficiency was 98–99%. The mapping efficiency was approximately 95%. This is significantly higher compared to other mapping software such as Bismark (Krueger and Andrews 2011). The total number of sequenced and mapped reads in all individual samples is provided in **Supplementary Table 1**. Among all the sequenced CpG sites, on average approximately 93% of them are methylated and 7% are unmethylated. The global CpG methylation level in DMSO treated group was 85% whereas in the two PCB126 exposed groups were 83% (**Figure 2**). The number of methylated and unmethylated CpG sites sequenced in each sample is provided in **Supplementary Table 2**.

PCB126 exposure induced changes in DNA methylation

BAT analysis predicted 308 differentially methylated regions (DMRs) in 3nM PCB126 exposed group but only 37 of them are statistically significant (adjusted p.value < 0.05; **Supplemental Figure 2A**). Among them 10 DMRs were hypermethylated and 27 of them were hypomethylated. The complete list of DMRs, their chromosomal coordinates and methylation levels in DMSO and 3nM PCB126 groups are provided in the supplementary information (3nM_PCB126_Metilene_DMRs.xlsx). Nine out of 37 DMRs are located in chromosome 4 and

majority of them are hypomethylated (7 out 9). Annotation of DMRs revealed that a majority of the DMRs are located in introns (20 DMRs), intergenic regions (8) and distal promoter regions (5). The remaining DMRs are located in the proximal promoters (3) and exons (one DMR) (**Figure 3A**). None of the DMRs overlapped with CpG islands and only one DMR was localized to a CpG shore (chr23:34148838 - 34148922). DMRs also overlapped with various repetitive elements (REs) with 19 DMRs associated with DNA repetitive elements, 4 DMRs with LTRs, 2 with LINE sequences and 12 with unannotated REs (**Figure 3B**).

In 10 nM PCB126 exposed group, 460 DMRs were predicted and 92 of them are statistically significant (adjusted p.value < 0.05; **Supplemental Figure 2B**). Among the 92 significant DMRs, 12 of them are hypermethylated and 80 DMRs hypomethylated. The complete list of DMRs, their chromosomal coordinates and methylation levels in DMSO and 10nM PCB126 groups are provided in the supplementary information (10nM_PCB126_Metilene_DMRs.xlsx). We observed 34 DMRs localized to chromosome 4 and 31 of them are hypomethylated. Annotation of DMRs revealed that majority of the DMRs are located in introns (36 DMRs), intergenic regions (36) and distal promoter regions (9). The remaining DMRs are located in the proximal promoters and exons (**Figure 3A**). Out of 92 DMRs, 6 of them overlapped with CpG islands and another 14 are located in the CpG shores. Majority of the DMRs overlapped with DNA (27), LTR (17) and rRNA (11) elements (**Figure 3B**).

We observed 19 DMRs to be common between the two PCB126 treatment groups. Among them 14 and 5 are hypomethylated and hypermethylated, respectively. (**Figure 4**).

Gene Ontology (GO) term analysis of statistically significant DMRs revealed overlap in the enriched terms between the two PCB126 treated groups. GO biological process (BP) parent term cellular pigmentation (GO:0033059) and all its child terms - pigment granule dispersal

(GO:0051876), pigment granule aggregation in cell center (GO:0051877), establishment of pigment granule localization (GO:0051905) and pigment granule localization (GO:0051875) are significantly enriched among the hypermethylated DMRs in 3nM PCB126 group (**Table 1**). In 10nM PCB126 group, hypermethylated DMRs are enriched in 2 pigment related GO terms as in 3nM PCB126 group (GO:0051876 and GO:0051877). In addition, cation transport (GO:0006812) and ATP biosynthetic process (GO:0006754) are represented (**Table 2**). Hypomethylated DMRs from 3 nM PCB126 group are enriched in GO BP terms related to RNA processing (3' RNA processing and RNA polyadenylation) and nucleoside metabolic process (GDP and ADP metabolic process) (**Table 1**). RNA processing terms are also enriched among hypomethylated DMRs from 10nM PCB126 group. In addition, iron-sulfur cluster assembly (GO:0016226), calcium-independent cell-cell adhesion (GO:0016338) and gluconeogenesis (GO:0006094) terms are enriched in 10nM PCB126 group (**Table 2**).

GO molecular function terms enriched among 3nM and 10nM PCB126 group hypermethylated DMRs include melatonin receptor activity and several ion channel activity terms. The hypomethylated DMRs are enriched in GO MF terms related to nucleotide transferase activity and ion binding activity in 3 and 10 nM PCB126 groups, respectively (**Tables 1 and 2**).

Transcriptional profiling

RNA sequencing revealed differential expression of 40 and 1621 genes in response to 3nM and 10 nM PCB126 exposure, respectively (5% FDR; **Figure 5**). Among the 40 differentially expressed genes in 3nM PCB126 group, 26 genes were upregulated and 14 downregulated. The upregulated DEGs represented in these GO terms are mainly classical AHR target genes such as *cyp1a, ahrra, tiparp* etc. Downregulated genes include extracellular matrix proteins and inflammatory response genes but there was no enrichment of GO terms.

PCB126 10nM exposure group showed differential expression of 1621 genes, with 1140 and 480 genes that were up and downregulated, respectively. Gene Ontology analysis of upregulated DEGs reveals enrichment of BP terms related to immune response and negative regulation of developmental process (**Figure 6A**) and MF terms cytokine receptor binding (**Figure 6B**). Downregulated DEGs are enriched in GO BP terms organelle organization, DNA repair and cell cycle process (**Figure 7A**) and GO MF terms protein binding and microtubule motor activity (**Figure 7B**).

There is a significant overlap between the two treatment groups. Out of 40 DEGs in 3nM PCB126 group, 34 of them are found in 10nM PCB126 group (**Table 3**). The complete annotated list of DEGs is provided in supplementary information (**DEGs.xlsx**).

Relationship between PCB126 induced DNA methylation and gene expression changes

We observed one DMR to be significantly correlated with gene expression in the 3nM PCB126 group (Spearman's rank correlation test adjusted p-value < 0.05). In 10 nM PCB126 group, 9 DMRs showed significant correlation with gene expression (**Table 4**). However, the classical inverse correlation between DNA methylation and gene expression was observed in 6 out of 9 DMRs (all in 10nM PCB126 group). A representative correlation plot showing inverse correlation between DNA methylation (DMR_69) and gene expression (ENSDARG00000089382) is shown (**Figure 8**).

Discussion

Our results demonstrate that PCB126 exposure altered DNA methylation and expression patterns of several genes involved in testicular development. It is well established that spermatogenesis is under the regulation of a complex network of steroid producing Leydig cells

and various other cell types. PCB126 exposure predominantly caused DNA hypomethylation and these regions are linked to the regulation of RNA processing, nucleotide metabolism and gluconeogenesis. We also observed a small number of hypermethylated DMR in response to PCB126 exposure and they are associated with regulating immune function and ion transporters. These results suggest that dioxin-like PCB exposure alters a variety of important functions associated with normal development of testis. However, these changes are not mediated by alterations in the expression of DNA methyltransferases, enzymes involved in the maintenance and establishment of DNA methylation, as we have shown previously in zebrafish embryos (Aluru et al. 2015). This suggests that dioxin-like PCBs target different regions of the genome for hypomethylation by recruiting DNA demethylation proteins and causing enzymatic oxidation of 5-methylcytosine as shown with TCDD exposure-induced AHR activation in rodents (Amenya et al. 2016) or by other mechanisms involving AHR as a reader and modulator of DNA methylation (Habano et al. 2022).

PCB126 exposure caused significant hypomethylation of DNA in zebrafish testis. These results are in agreement with previous experimental studies where dioxin and dioxin-like PCBs exposure have been shown to cause DNA hypomethylation (Pittman et al., 2020; Vidali et al. 2021). It has been widely established that there are extremely high levels of transcription in testicular cells and the high gene expression levels have been shown to be epigenetically regulated by DNA methylation and histone modifications in meiotic and postmeiotic spermatogenic cells (Soumillon et al. 2013). Gene Ontology analysis of hypomethylated DMRs revealed that these regions are associated with RNA processing (post-transcriptional regulation), nucleic acid metabolism and energy metabolism (gluconeogenesis).

During spermatogenesis, post-transcriptional regulation is an important process as the germ cells experience extended periods of inactive transcription despite heavy translational

requirements for continued differentiation and growth (Bettegowda and Wilkinson 2010). Any perturbation to these mechanisms of posttranscriptional control during spermatogenesis could result in nonviable gametes (Braun 1998; Idler et al. 2012). One of the main players in the post-transcriptional regulation are RNA binding proteins (RBPs), an extensive group of proteins that recognize and bind to specific sequences of RNA, and regulate their function (Sutherland et al. 2015). RBPs are highly expressed throughout spermatogenesis and have been well documented as being essential to posttranscriptional control during all stages of germ cell development (Paronetto and Sette 2010). Our RNAseq results show upregulation of several nuclear and cytoplasmic RBPs in response to PCB126 exposure (*rbm14a, rbm11, rbm38, rbm46, rbms2b, hnrnp0a*). Nuclear RBPs such as *rbm11, 14a, 38* and *46* regulate nascent mRNA (pre-mRNA) processing, including capping, polyadenylation, and splicing. Whereas cytoplasmic RBPs bind mature mRNA sequences in the cytoplasm and direct mRNA transport, competitive or co-operative interactions with translation machinery, and regulating mRNA stability. Aberrant expression of RBPs has been shown to result in spermatogenic arrest and sterility (Cooke and Elliott 1997; Yang et al. 2005; Zheng et al. 2021). Recent studies have demonstrated that N6-methyladenosine (m6A) modified messenger RNAs (mRNAs) interact with RBPs and regulate diverse processes including meiosis, DNA damage response, and germ cell and neuronal development (Kasowitz et al. 2018; Tang et al. 2018; Wang et al. 2018; Wojtas et al. 2017; Xiang et al. 2017). We recently demonstrated that developmental exposure of zebrafish embryos to PCB126 altered m6A patterns in several mRNA transcripts, suggesting that environmental chemicals can interfere with epitranscriptomic processes (Aluru and Karchner 2021). Further work needs to be done to investigate the cross talk between DNA methylation and epitranscriptomics and the potential role of environmental chemicals in affecting this crosstalk.

Another GO pathway significantly enriched among the hypomethylated DMRs is the nucleoside metabolic process. Nucleosides are essential for nucleotide synthesis during spermatogenesis and are supplied to the germ cells via tight junctions from the somatic sertoli cells (Bart et al. 2002). Adenosine, a purine nucleoside has been shown to be required for acquisition of sperm motility (Aitken et al. 1986; Gerton et al. 2009). One of the genes represented in this GO term is a NUDIX hydrolase (nudt18), an enzyme that carries out hydrolysis reactions, substrates of which include dNTPs, non-nucleoside polyphosphates, and capped mRNAs (Carreras-Puigvert et al. 2017; Mildvan et al. 2005). NUDIX enzymes have been shown to be upregulated in response to cellular (oxidative) stress and are involved in clearing the cells of deleterious metabolites, such as oxidized nucleotides, ensuring proper cell homeostasis. It is not surprising based on the evidence that PCB126 induces oxidative stress genes (Aluru et al., 2018). Our gene expression analysis shows upregulation of several oxidative stress genes (e.g., *gstk1,gstt1b,gsto2, gsta2, nfe2l2a, nrros*). We also observed *nudt18* to be moderately upregulated in 10nM PCB126 group but it is not statistically significant (log2FC 0.2, FDR 0.5%). These results suggest that PCB126 exposure induced cellular stress in the testis and some of the genes involved in maintaining cellular homeostasis are regulated by DNA methylation.

In addition, some of the hypomethylated DMRs seem to regulate genes associated with Iron–sulfur (Fe–S) cluster assembly, small inorganic structures constituting the catalytic site of a multitude of enzymes including cytochrome P450s. It is not surprising given the fact that PCB126 induces the expression of several cytochrome P450s and we observed upregulation of several phase I and phase II biotransformation enzymes that are dependent on Fe-S protein, Ferredoxin. These results suggest that some of the fundamental players in xenobiotic metabolism are under epigenetic regulation.

Interestingly, a significant number of DMRs in both 3 and 10 nM PCB126 treated groups are located in chromosome 4, a unique genomic region in the zebrafish genome with extensive heterochromatin, presence of repetitive elements and lack of protein coding genes (Howe et al. 2013). In addition, majority of the genes present on chromosome 4 are unique to zebrafish and do not have human orthologs. Considering the presence of high levels of DNA methylation in the heterochromatic region (Richards and Elgin 2002), it is not surprising that PCB126 exposure altered methylation patterns in this genomic region. The consequences of hypomethylation in this region could have serious consequences on genome stability as repetitive elements can move from one location to another. Further studies are needed to understand the consequences of hypomethylation in this chromosome.

Even though majority of the DMRs were hypomethylated, PCB126 exposure also caused hypermethylation of few genomic regions. Functional annotation of these DMRs suggest enrichment of regions that regulate cellular pigmentation, particularly melatonin receptor activity. It is not surprising given the evolutionarily conserved role of melatonin in the regulation of hypothalamus-pituitary-testicular axis. Melatonin secreted by the pineal gland not only regulates testicular function by acting on the hypothalamus and the anterior pituitary, but is also taken up by the testis where it has been shown to modulate testicular activity (Frungieri et al. 2017). In addition, testes has also been shown to synthesize melatonin (Gonzalez-Arto et al. 2016; Tijmes et al. 1996), where it modulates cellular growth, proliferation, and testosterone secretion by several testicular cell types. Melatonin also protects the testis against inflammation and reactive oxygen species (ROS) from toxicant induced oxidative stress. In fact, low melatonin levels have been associated with reduced sperm motility and abnormal sperm progression (Rossi et al. 2014). Hypermethylation of regions that regulate genes associated with melatonin secretion and activity could prevent local inflammatory and oxidative stress responses leading to defects in testicular function and potential infertility.

We observed classical responses to PCB126 exposure where genes associated with xenobiotic metabolism were upregulated. Almost all of these are AHR target genes and have been shown previously to be altered by dioxins and dioxin-like PCBs in a variety of animals including zebrafish (Aluru et al. 2017; Aluru et al., 2018). These core set genes were upregulated in both 3 and 10 nM PCB126 exposed groups. In addition to the core set, we only observed very few genes differentially expressed with 3nM PCB126 exposure. In contrast, we observed more than 1600 DEGs in response to 10nM PCB126 exposure. This is not surprising given the fact that exposure to high concentrations of dioxin or dioxin-like PCBs alters the expression of genes belonging to multiple physiological pathways and many of these changes could be secondary and tertiary responses to exposure. Nevertheless, gene ontology term analysis suggests that many of the upregulated genes are associated with immune function. Testis is considered an immune privileged organ with tightest of all blood-tissue barriers in majority of vertebrates (Cheng and Mruk 2012; Zhao et al. 2014). The blood-testis barrier protects immunogenic germ cells from systemic immune attack, and impairment of immune homeostasis in the testis can result in male infertility. Several environmental toxicants have been shown to disturb the blood-testis barrier integrity by affecting the tight and gap junctions (Cheng and Mruk 2012). One recent study has demonstrated that developmental exposure to TCDD induces testicular inflammation (increase in macrophages) and this correlated with reduced fertility (Bruner-Tran et al. 2014). Our results suggest that several genes associated with innate immune system are upregulated suggesting that high concentrations of PCB126 exposure adversely impacts immune homeostasis in the testis. In addition, exposure to this concentration downregulated genes that are critical for proper sperm development. Further studies need to be conducted to determine if preconceptual exposure to environmentally relevant concentrations of PCB126 (such as 3 nM used in this study) will affect sperm motility and fertilization success.

With regard to correlation between DNA methylation changes and differential gene expression, our results suggest a complex relationships with considerable involvement of chromatin modifications. Although most DMRs seem unrelated to gene expression, a small proportion of them showed classical inverse relationship between gene expression and DNA methylation. Interestingly, the properties of these relationships appear quite complex, and the distance between the DMR and the transcriptional start site provides relatively little information about the sign of the correlation. To understand the roles of DMRs on gene expression, approaches such as chromosome confirmation capture techniques (Hi-C) should be used to obtain high resolution conformational features such as DNA loops. Despite very little correlation between DNA methylation and gene expression, the alterations observed in these end points suggest that PCB126 exposure significantly affects important players in testicular development and function.

Conclusions

In this study, we demonstrated that paternal preconception exposure to dioxin-like PCBs cause concentration-dependent genome wide DNA hypomethylation in the developing germ cells. These findings may have important implications to reproductive outcomes as majority of the DMRs identified seems to regulate genes essential for spermatogenesis. Although future studies should investigate the impacts of altered sperm DNA methylation on fertilization success and embryo survival, the DMRs identified in this study may be good candidates to investigate the role of DNA methylation in multigenerational effects of preconception exposure to dioxin-like PCBs. Majority of the DMRs identified in this study are located in the intergenic regions and their role in gene regulation needs to be experimentally validated. The availability of tools such as Hi-C will help in assigning distant regulatory regions to their target genes, which is essential for understanding the regulation of gene expression.

Acknowledgements

The authors would like to acknowledge the help provided by Dr. Michael Moore with analysis of histology sections.

Funding

National Institute of Environmental Health Sciences (NIH R01ES024915); Woods Hole Center for Oceans and Human Health (NIH/NIEHS Grant P01ES028938); National Science Foundation (Grant OCE-1840381). JE was supported by DFG grants to Peter F. Stadler and by Joachim Herz Stiftung.

References

Aitken, R. J., Mattei, A., and Irvine, S. 1986. Paradoxical stimulation of human sperm motility by 2-deoxyadenosine. J Reprod Fertil 78(2), 515-27.

Akemann, C., Meyer, D. N., Gurdziel, K., and Baker, T. R. 2020. TCDD-induced multi- and transgenerational changes in the methylome of male zebrafish gonads. Environ Epigenet 6(1), dvaa010.

Aluru, N., and Engelhardt, J. 2022. Exposure to 3, 3', 4, 4', 5-pentachlorobiphenyl (PCB 126) causes widespread DNA hypomethylation in adult zebrafish testis. https://doi.org/10.5061/dryad.7pvmcvdw1.

Aluru, N., and Karchner, S. I. 2021. PCB126 Exposure Revealed Alterations in m6A RNA Modifications in Transcripts Associated With AHR Activation. Toxicol Sci 179(1), 84-94.

Aluru, N., Karchner, S. I., and Glazer, L. 2017. Early Life Exposure to Low Levels of AHR Agonist PCB126 (3,3',4,4',5-Pentachlorobiphenyl) Reprograms Gene Expression in Adult Brain. Toxicol Sci 160(2), 386-397.

Aluru, N., Karchner, S. I., Krick, K. S., Zhu, W., and Liu, J. 2018. Role of DNA methylation in altered gene expression patterns in adult zebrafish (*Danio rerio*) exposed to 3, 3', 4, 4', 5-pentachlorobiphenyl (PCB 126). Environ Epigenet 4(1), dvy005.

Aluru, N., Kuo, E., Helfrich, L. W., Karchner, S. I., Linney, E. A., Pais, J. E., and Franks, D. G. 2015. Developmental exposure to 2,3,7,8-tetrachlorodibenzo-p-dioxin alters DNA methyltransferase (dnmt) expression in zebrafish (*Danio rerio*). Toxicol Appl Pharmacol 284(2), 142-51.

Amenya, H. Z., Tohyama, C., and Ohsako, S. 2016. Dioxin induces Ahr-dependent robust DNA demethylation of the Cyp1a1 promoter via Tdg in the mouse liver. Sci Rep 6, 34989.

Anders, S., Pyl, P. T., and Huber, W. 2015. HTSeq--a Python framework to work with high-throughput sequencing data. Bioinformatics 31(2), 166-9.

Andrews, S. (2010). FastQC: A quality control tool for high throughput sequence data [online]. Available online at: http://www.bioinformatics.babraham.ac.uk/projects/fastqc.

Avilla, M. N., Malecki, K. M. C., Hahn, M. E., Wilson, R. H., and Bradfield, C. A. 2020. The Ah Receptor: Adaptive Metabolism, Ligand Diversity, and the Xenokine Model. Chem Res Toxicol 33(4), 860-879.

Bart, J., Groen, H. J., van der Graaf, W. T., Hollema, H., Hendrikse, N. H., Vaalburg, W., Sleijfer, D. T., and de Vries, E. G. 2002. An oncological view on the blood-testis barrier. Lancet Oncol 3(6), 357-63.

Benjamini, Y., and Hochberg, Y. 1995. Controlling the False Discovery Rate: A Practical and Powerful Approach to Multiple Testing. Journal of the Royal Statistical Society. Series B (Methodological) 57(1), 289-300.

Bettegowda, A., and Wilkinson, M. F. 2010. Transcription and post-transcriptional regulation of spermatogenesis. Philos Trans R Soc Lond B Biol Sci 365(1546), 1637-51.

Braun, R. E. 1998. Post-transcriptional control of gene expression during spermatogenesis. Semin Cell Dev Biol 9(4), 483-9.

Bruner-Tran, K. L., Ding, T., Yeoman, K. B., Archibong, A., Arosh, J. A., and Osteen, K. G. 2014. Developmental exposure of mice to dioxin promotes transgenerational testicular inflammation and an increased risk of preterm birth in unexposed mating partners. PLoS One 9(8), e105084.

Carreras-Puigvert, J., Zitnik, M., Jemth, A. S., Carter, M., Unterlass, J. E., Hallstrom, B., Loseva, O., Karem, Z., Calderon-Montano, J. M., Lindskog, C., Edqvist, P. H., Matuszewski, D. J., Ait Blal, H., Berntsson, R. P. A., Haggblad, M., Martens, U., Studham, M., Lundgren, B., Wahlby, C., Sonnhammer, E. L. L., Lundberg, E., Stenmark, P., Zupan, B., and Helleday, T. 2017. A comprehensive structural, biochemical and biological profiling of the human NUDIX hydrolase family. Nat Commun 8(1), 1541.

Cheng, C. Y., and Mruk, D. D. 2012. The blood-testis barrier and its implications for male contraception. Pharmacol Rev 64(1), 16-64.

Cooke, H. J., and Elliott, D. J. 1997. RNA-binding proteins and human male infertility. Trends Genet 13(3), 87-9.

Coulter, D. P., Huff Hartz, K. E., Sepulveda, M. S., Godfrey, A., Garvey, J. E., and Lydy, M. J. 2019. Lifelong Exposure to Dioxin-Like PCBs Alters Paternal Offspring Care Behavior and Reduces Male Fish Reproductive Success. Environ Sci Technol 53(19), 11507-11514.

Day, J., Savani, S., Krempley, B. D., Nguyen, M., and Kitlinska, J. B. 2016. Influence of paternal preconception exposures on their offspring: through epigenetics to phenotype. Am J Stem Cells 5(1), 11-8.

Faroon, O., and Ruiz, P. 2016. Polychlorinated biphenyls: New evidence from the last decade. Toxicol Ind Health 32(11), 1825-1847.

Frungieri, M. B., Calandra, R. S., and Rossi, S. P. 2017. Local Actions of Melatonin in Somatic Cells of the Testis. Int J Mol Sci 18(6).

Gerton, G. L., Aghajanian, H. K., Haig-Ladewig, L., and Cao, W. 2009. Adenine Nucleotides and Sperm Motility.George L. Gerton, Ph.D. Biology of Reproduction 81(Suppl_1), 14-14.

Gonzalez-Arto, M., Hamilton, T. R., Gallego, M., Gaspar-Torrubia, E., Aguilar, D., Serrano-Blesa, E., Abecia, J. A., Perez-Pe, R., Muino-Blanco, T., Cebrian-Perez, J. A., and Casao, A. 2016. Evidence of melatonin synthesis in the ram reproductive tract. Andrology 4(1), 163-71.

Habano, W., Miura, T., Terashima, J., and Ozawa, S. 2022. Aryl hydrocarbon receptor as a DNA methylation reader in the stress response pathway. Toxicology 470, 153154.

Heindel, J. J. 2019. The developmental basis of disease: Update on environmental exposures and animal models. Basic Clin Pharmacol Toxicol 125 Suppl 3, 5-13.

Howe, K., Clark, M. D., Torroja, C. F., Torrance, J., Berthelot, C., Muffato, M., Collins, J. E., Humphray, S., McLaren, K., Matthews, L., McLaren, S., Sealy, I., Caccamo, M., Churcher, C., Scott, C., Barrett, J. C., Koch, R., Rauch, G. J., White, S., Chow, W., Kilian, B., Quintais, L. T., Guerra-Assuncao, J. A., Zhou, Y., Gu, Y., Yen, J., Vogel, J. H., Eyre, T., Redmond, S., Banerjee, R., Chi, J., Fu, B., Langley, E., Maguire, S. F., Laird, G. K., Lloyd, D., Kenyon, E., Donaldson, S., Sehra, H., Almeida-King, J., Loveland, J., Trevanion, S., Jones, M., Quail, M., Willey, D., Hunt, A., Burton, J., Sims, S., McLay, K., Plumb, B., Davis, J., Clee, C., Oliver, K., Clark, R., Riddle, C., Elliot, D., Threadgold, G., Harden, G., Ware, D., Begum, S., Mortimore, B., Kerry, G., Heath, P., Phillimore, B., Tracey, A., Corby, N., Dunn, M., Johnson, C., Wood, J., Clark, S., Pelan, S., Griffiths, G., Smith, M., Glithero, R., Howden, P., Barker, N., Lloyd, C., Stevens, C., Harley, J., Holt, K., Panagiotidis, G., Lovell, J., Beasley, H., Henderson, C., Gordon, D., Auger, K., Wright, D., Collins, J., Raisen, C., Dyer, L., Leung, K., Robertson, L., Ambridge, K., Leongamornlert, D., McGuire, S., Gilderthorp, R., Griffiths, C., Manthravadi, D., Nichol, S., Barker, G., Whitehead, S., Kay, M., Brown, J., Murnane, C., Gray, E., Humphries, M., Sycamore, N., Barker, D., Saunders, D., Wallis, J., Babbage, A., Hammond, S., Mashreghi-Mohammadi, M., Barr, L., Martin, S., Wray, P., Ellington, A., Matthews, N., Ellwood, M., Woodmansey, R., Clark, G., Cooper, J., Tromans, A., Grafham, D., Skuce, C., Pandian, R., Andrews, R., Harrison, E., Kimberley, A., Garnett, J., Fosker, N., Hall, R., Garner, P., Kelly, D., Bird, C., Palmer, S., Gehring, I., Berger, A., Dooley, C. M., Ersan-Urun, Z., Eser, C., Geiger, H., Geisler, M., Karotki, L., Kirn, A., Konantz, J., Konantz, M., Oberlander, M., Rudolph-Geiger, S., Teucke, M., Lanz, C., Raddatz, G., Osoegawa, K., Zhu, B., Rapp, A., Widaa, S., Langford, C., Yang, F., Schuster, S. C., Carter, N. P., Harrow, J., Ning, Z., Herrero, J., Searle, S. M., Enright, A., Geisler, R., Plasterk, R. H., Lee, C., Westerfield, M., de Jong, P. J., Zon, L. I., Postlethwait, J. H., Nusslein-Volhard, C., Hubbard, T. J., Roest Crollius, H., Rogers, J., and Stemple, D. L. 2013. The zebrafish reference genome sequence and its relationship to the human genome. Nature 496(7446), 498-503.

Idler, R. K., Hennig, G. W., and Yan, W. 2012. Bioinformatic identification of novel elements potentially involved in messenger RNA fate control during spermatogenesis. Biol Reprod 87(6), 138.

Juhling, F., Kretzmer, H., Bernhart, S. H., Otto, C., Stadler, P. F., and Hoffmann, S. 2016. metilene: fast and sensitive calling of differentially methylated regions from bisulfite sequencing data. Genome Res 26(2), 256-62.

Kasowitz, S. D., Ma, J., Anderson, S. J., Leu, N. A., Xu, Y., Gregory, B. D., Schultz, R. M., and Wang, P. J. 2018. Nuclear m6A reader YTHDC1 regulates alternative polyadenylation and splicing during mouse oocyte development. PLoS Genet 14(5), e1007412.

Khanjani, N., and Sim, M. R. 2007. Maternal contamination with PCBs and reproductive outcomes in an Australian population. J Expo Sci Environ Epidemiol 17(2), 191-5.

Kim, K. Y., Kim, D. S., Lee, S. K., Lee, I. K., Kang, J. H., Chang, Y. S., Jacobs, D. R., Steffes, M., and Lee, D. H. 2010. Association of low-dose exposure to persistent organic pollutants with global DNA hypomethylation in healthy Koreans. Environ Health Perspect 118(3), 370-4.

Kretzmer, H., Otto, C., and Hoffmann, S. 2017. BAT: Bisulfite Analysis Toolkit: BAT is a toolkit to analyze DNA methylation sequencing data accurately and reproducibly. It covers standard processing and analysis steps from raw read mapping up to annotation data integration and calculation of correlating DMRs. F1000Res 6, 1490.

Krueger, F., and Andrews, S. R. 2011. Bismark: a flexible aligner and methylation caller for Bisulfite-Seq applications. Bioinformatics 27(11), 1571-2.

Kuznetsova, I., Lugmayr, A., Siira, S. J., Rackham, O., and Filipovska, A. 2019. CirGO: an alternative circular way of visualising gene ontology terms. BMC Bioinformatics 20(1), 84.

Lauby-Secretan, B., Loomis, D., Baan, R., El Ghissassi, F., Bouvard, V., Benbrahim-Tallaa, L., Guha, N., Grosse, Y., and Straif, K. 2016. Use of mechanistic data in the IARC evaluations of the carcinogenicity of polychlorinated biphenyls and related compounds. Environ Sci Pollut Res Int 23(3), 2220-9.

Lind, L., Penell, J., Luttropp, K., Nordfors, L., Syvanen, A. C., Axelsson, T., Salihovic, S., van Bavel, B., Fall, T., Ingelsson, E., and Lind, P. M. 2013. Global DNA hypermethylation is associated with high serum levels of persistent organic pollutants in an elderly population. Environ Int 59, 456-61.

Liu, Y., Han, Y., Zhou, L., Pan, X., Sun, X., Liu, Y., Liang, M., Qin, J., Lu, Y., and Liu, P. 2020. A comprehensive evaluation of computational tools to identify differential methylation regions using RRBS data. Genomics 112(6), 4567-4576.

Love, M. I., Huber, W., and Anders, S. 2014. Moderated estimation of fold change and dispersion for RNA-seq data with DESeq2. Genome Biol 15(12), 550.

Manikkam, M., Tracey, R., Guerrero-Bosagna, C., and Skinner, M. K. 2012. Dioxin (TCDD) induces epigenetic transgenerational inheritance of adult onset disease and sperm epimutations. PLoS One 7(9), e46249.

McLean, C. Y., Bristor, D., Hiller, M., Clarke, S. L., Schaar, B. T., Lowe, C. B., Wenger, A. M., and Bejerano, G. 2010. GREAT improves functional interpretation of cis-regulatory regions. Nat Biotechnol 28(5), 495-501.

Meeker, J. D., and Hauser, R. 2010. Exposure to polychlorinated biphenyls (PCBs) and male reproduction. Syst Biol Reprod Med 56(2), 122-31.

Mildvan, A. S., Xia, Z., Azurmendi, H. F., Saraswat, V., Legler, P. M., Massiah, M. A., Gabelli, S. B., Bianchet, M. A., Kang, L. W., and Amzel, L. M. 2005. Structures and mechanisms of Nudix hydrolases. Arch Biochem Biophys 433(1), 129-43.

Mocarelli, P., Gerthoux, P. M., Needham, L. L., Patterson, D. G., Jr., Limonta, G., Falbo, R., Signorini, S., Bertona, M., Crespi, C., Sarto, C., Scott, P. K., Turner, W. E., and Brambilla, P. 2011. Perinatal exposure to low doses of dioxin can permanently impair human semen quality. Environ Health Perspect 119(5), 713-8.

Paronetto, M. P., and Sette, C. 2010. Role of RNA-binding proteins in mammalian spermatogenesis. Int J Androl 33(1), 2-12.

Pittman, G. S., Wang, X., Campbell, M. R., Coulter, S. J., Olson, J. R., Pavuk, M., Birnbaum, L. S., and Bell, D. A. 2020. Dioxin-like compound exposures and DNA methylation in the Anniston Community Health Survey Phase II. Sci Total Environ 742, 140424.

Reimand, J., Arak, T., Adler, P., Kolberg, L., Reisberg, S., Peterson, H., and Vilo, J. 2016. g:Profiler-a web server for functional interpretation of gene lists (2016 update). Nucleic Acids Res 44(W1), W83-9.

Richards, E. J., and Elgin, S. C. 2002. Epigenetic codes for heterochromatin formation and silencing: rounding up the usual suspects. Cell 108(4), 489-500.

Rossi, S. P., Windschuettl, S., Matzkin, M. E., Terradas, C., Ponzio, R., Puigdomenech, E., Levalle, O., Calandra, R. S., Mayerhofer, A., and Frungieri, M. B. 2014. Melatonin in testes of infertile men: evidence for anti-proliferative and anti-oxidant effects on local macrophage and mast cell populations. Andrology 2(3), 436-49.

Ruiz-Hernandez, A., Kuo, C. C., Rentero-Garrido, P., Tang, W. Y., Redon, J., Ordovas, J. M., Navas-Acien, A., and Tellez-Plaza, M. 2015. Environmental chemicals and DNA methylation in adults: a systematic review of the epidemiologic evidence. Clin Epigenetics 7, 55.

Rusiecki, J. A., Baccarelli, A., Bollati, V., Tarantini, L., Moore, L. E., and Bonefeld-Jorgensen, E. C. 2008. Global DNA hypomethylation is associated with high serum-persistent organic pollutants in Greenlandic Inuit. Environ Health Perspect 116(11), 1547-52.

Safe, S. 1990. Polychlorinated biphenyls (PCBs), dibenzo-p-dioxins (PCDDs), dibenzofurans (PCDFs), and related compounds: environmental and mechanistic considerations which support the development of toxic equivalency factors (TEFs). Crit Rev Toxicol 21(1), 51-88.

Segal, T. R., and Giudice, L. C. 2019. Before the beginning: environmental exposures and reproductive and obstetrical outcomes. Fertil Steril 112(4), 613-621.

Soumillon, M., Necsulea, A., Weier, M., Brawand, D., Zhang, X., Gu, H., Barthes, P., Kokkinaki, M., Nef, S., Gnirke, A., Dym, M., de Massy, B., Mikkelsen, T. S., and Kaessmann, H. 2013. Cellular source and mechanisms of high transcriptome complexity in the mammalian testis. Cell Rep 3(6), 2179-90.

Supek, F., Bosnjak, M., Skunca, N., and Smuc, T. 2011. REVIGO summarizes and visualizes long lists of gene ontology terms. PLoS One 6(7), e21800.

Sutherland, J. M., Siddall, N. A., Hime, G. R., and McLaughlin, E. A. 2015. RNA binding proteins in spermatogenesis: an in depth focus on the Musashi family. Asian J Androl 17(4), 529-36.
Tang, C., Klukovich, R., Peng, H., Wang, Z., Yu, T., Zhang, Y., Zheng, H., Klungland, A., and Yan, W. 2018. ALKBH5-dependent m6A demethylation controls splicing and stability of long 3'-UTR mRNAs in male germ cells. Proc Natl Acad Sci U S A 115(2), E325-E333.

Tellez-Plaza, M., Tang, W. Y., Shang, Y., Umans, J. G., Francesconi, K. A., Goessler, W., Ledesma, M., Leon, M., Laclaustra, M., Pollak, J., Guallar, E., Cole, S. A., Fallin, M. D., and Navas-Acien, A. 2014. Association of global DNA methylation and global DNA hydroxymethylation with metals and other exposures in human blood DNA samples. Environ Health Perspect 122(9), 946-54.

Tijmes, M., Pedraza, R., and Valladares, L. 1996. Melatonin in the rat testis: evidence for local synthesis. Steroids 61(2), 65-8.

Venkatratnam, A., Douillet, C., Topping, B. C., Shi, Q., Addo, K. A., Ideraabdullah, F. Y., Fry, R. C., and Styblo, M. 2021. Sex-dependent effects of preconception exposure to arsenite on gene transcription in parental germ cells and on transcriptomic profiles and diabetic phenotype of offspring. Arch Toxicol 95(2), 473-488.

Vidali, M. S., Dailianis, S., Vlastos, D., and Georgiadis, P. 2021. PCB cause global DNA hypomethylation of human peripheral blood monocytes in vitro. Environ Toxicol Pharmacol 87, 103696.

Viluksela, M., and Pohjanvirta, R. 2019. Multigenerational and Transgenerational Effects of Dioxins. Int J Mol Sci 20(12).

Wang, C. X., Cui, G. S., Liu, X., Xu, K., Wang, M., Zhang, X. X., Jiang, L. Y., Li, A., Yang, Y., Lai, W. Y., Sun, B. F., Jiang, G. B., Wang, H. L., Tong, W. M., Li, W., Wang, X. J., Yang, Y. G., and Zhou, Q. 2018. METTL3-mediated m6A modification is required for cerebellar development. PLoS Biol 16(6), e2004880.

Wojtas, M. N., Pandey, R. R., Mendel, M., Homolka, D., Sachidanandam, R., and Pillai, R. S. 2017. Regulation of m(6)A Transcripts by the 3'-->5' RNA Helicase YTHDC2 Is Essential for a Successful Meiotic Program in the Mammalian Germline. Mol Cell 68(2), 374-387 e12.

Xiang, Y., Laurent, B., Hsu, C. H., Nachtergaele, S., Lu, Z., Sheng, W., Xu, C., Chen, H., Ouyang, J., Wang, S., Ling, D., Hsu, P. H., Zou, L., Jambhekar, A., He, C., and Shi, Y. 2017. RNA m(6)A methylation regulates the ultraviolet-induced DNA damage response. Nature 543(7646), 573-576.

Xue, J., Liu, S. V., Zartarian, V. G., Geller, A. M., and Schultz, B. D. 2014. Analysis of NHANES measured blood PCBs in the general US population and application of SHEDS model to identify key exposure factors. J Expo Sci Environ Epidemiol 24(6), 615-21.

Yang, A. S., Estecio, M. R., Doshi, K., Kondo, Y., Tajara, E. H., and Issa, J. P. 2004. A simple method for estimating global DNA methylation using bisulfite PCR of repetitive DNA elements. Nucleic Acids Res 32(3), e38.

Yang, J., Medvedev, S., Yu, J., Tang, L. C., Agno, J. E., Matzuk, M. M., Schultz, R. M., and Hecht, N. B. 2005. Absence of the DNA-/RNA-binding protein MSY2 results in male and female infertility. Proc Natl Acad Sci U S A 102(16), 5755-60.

Zhang, Y., Mustieles, V., Yland, J., Braun, J. M., Williams, P. L., Attaman, J. A., Ford, J. B., Calafat, A. M., Hauser, R., and Messerlian, C. 2020. Association of Parental Preconception Exposure to Phthalates and Phthalate Substitutes With Preterm Birth. JAMA Netw Open 3(4), e202159.

Zhao, S., Zhu, W., Xue, S., and Han, D. 2014. Testicular defense systems: immune privilege and innate immunity. Cell Mol Immunol 11(5), 428-37.

Zheng, M., Chen, X., Cui, Y., Li, W., Dai, H., Yue, Q., Zhang, H., Zheng, Y., Guo, X., and Zhu, H. 2021. TULP2, a New RNA-Binding Protein, Is Required for Mouse Spermatid Differentiation and Male Fertility. Front Cell Dev Biol 9, 623738.

List of figures

Figure 1. PCB126-induced *cyp1a* gene expression in the testis. *Cyp1a* expression was quantified using real-time quantitative PCR and relative expression was calculated using the delta Ct method. β-Actin was used as a reference gene. Values represent mean + SD (one-way ANOVA; n = 5-6). * Represents significant difference from DMSO control ($P < 0.01$).

Figure 2. Global CpG methylation levels in different treatment groups. The lower end of the box shows the first quartile, the line the median and the upper end of the box the third quartile. The upper whisker extends to the highest data point within 1.5 * IQR (IQR: the distance between first and third quartile), the lower whisker to the respective lowest data point. The point shows an outlier which is defined as a data point further away than the whiskers. These levels were determined from RRBS sample analysis. The detailed methods are provided in the materials and methods section. No significant difference in global DNA methylation was observed ($P < 0.01$; n=5-6).

Figure 3. Annotation of DMRs based on their genomic location (A) and repetitive elements (B). A. DMRs are classified into genomic locations (exons, introns, proximal promoters (PP), distal promoters (DP), intergenic regions (IGR), CpG islands (CpGi) and CpG shores (CpGs)). B. DMRs are classified based on their overlap with repetitive elements (DNA repeats, long terminal repeats (LTRs) and non-LTR elements (Long Interspersed Nuclear Elements (LINEs) or Short Interspersed Nuclear Elements (SINEs)). Genomic location and repetitive elements were identified using the zebrafish genome annotations available in the UCSC genome table browser.

Figure 4. Differentially methylated regions (DMRs) that are common to 3 nM and 10 nM PCB126 treatment groups.

Figure 5. Heatmap representation of differentially expressed genes in response to PCB126 exposure. Normalized read counts were used to plot the heat map.

Figure 6. Gene Ontology term visualization of biological process (A) and molecular function (B) terms from enrichment analysis of high PCB-exposure induced upregulated genes. The enriched GO BP and MF terms and the adjusted p.values were obtained from gProfiler were used as input in REVIGO. A semantic similarity threshold of 0.7 was used to remove redundant GO terms. Summarization and visualization of GO terms was carried out using CirGO software. The detailed methods are provided in the materials and methods section.

Figure 7. Gene Ontology term visualization of biological process (A) and molecular function (B) terms from enrichment analysis of high PCB-exposure induced downregulated genes. The enriched GO BP and MF terms and the adjusted p.values were obtained from gProfiler were used as input in REVIGO. A semantic similarity threshold of 0.7 was used to remove redundant GO terms. Summarization and visualization of GO terms was carried out using CirGO software. The detailed methods are provided in the materials and methods section.

Figure 8. Representative correlation plot showing a boxplot and scatterplot of mean methylation (DMR_69) and expression (ENSDARG00000089382; zgc:158463) values including the regression line (Spearman's rank correlation).

List of tables

Table 1. Gene Ontology (GO) terms represented among DMRs in 3nM PCB126 group.

GO Biological Process	GO ID	Adjusted p.value
Hypermethylated DMRs		
Pigment granule dispersal	GO:0051876	< 0.0001
Pigment granule aggregation in cell center	GO:0051877	< 0.0001
Establishment of pigment granule localization	GO:0051905	0.0002
Pigment granule localization	GO:0051875	0.0003
Cellular pigmentation	GO:0033059	0.0003
Hypomethylated DMRs		
RNA polyadenylation	GO:0043631	0.0002
RNA 3'-end processing	GO:0031123	0.0004
dADP catabolic process	GO:0046057	0.0014
dGDP catabolic process	GO:0046067	0.0014
GDP catabolic process	GO:0046712	0.0014
GO Molecular Function		
Hypermethylated DMRs		
Melatonin receptor activity	GO:0008502	0.0001
Inward rectifier potassium channel activity	GO:0005242	0.0003
Voltage-gated potassium channel activity	GO:0005249	0.0056
Potassium channel activity	GO:0005267	0.0087
Potassium ion transmembrane transporter activity	GO:0015079	0.0088
Hypomethylated DMRs		
Polynucleotide adenylyltransferase activity	GO:0004652	0.0001
Adenylyltransferase activity	GO:0070566	0.0004
8-oxo-dGDP phosphatase activity	GO:0044715	0.0011
8-oxo-GDP phosphatase activity	GO:0044716	0.0011
8-hydroxy-dADP phosphatase activity	GO:0044717	0.0011

Table 2. Gene Ontology (GO) terms represented among DMRs in 10nM PCB126 group.

GO Biological Process	GO ID	Adjusted p.value
Hypermethylated DMRs		
Monovalent inorganic cation transport	GO:0015672	< 0.0001
Pigment granule dispersal	GO:0051876	< 0.0001
Pigment granule aggregation in cell center	GO:0051877	< 0.0001
Cation transport	GO:0006812	0.0002
ATP biosynthetic process	GO:0006754	0.0003
Hypomethylated DMRs		
RNA polyadenylation	GO:0043631	0.0015
Iron-sulfur cluster assembly	GO:0016226	0.0023
Calcium-independent cell-cell adhesion	GO:0016338	0.003
RNA 3'-end processing	GO:0031123	0.0032
Gluconeogenesis	GO:0006094	0.0048
GO Molecular Function		
Hypermethylated DMRs		
Monovalent inorganic cation transmembrane transporter activity	GO:0015077	< 0.0001
Inorganic cation transmembrane transporter activity	GO:0022890	0.0001
Melatonin receptor activity	GO:0008502	0.0002
Cation transmembrane transporter activity	GO:0008324	0.0003
Inward rectifier potassium channel activity	GO:0005242	0.0005
Hypomethylated DMRs		
Ion binding	GO:0043167	< 0.0001
Nucleic acid binding	GO:0003676	< 0.0001
Metal ion binding	GO:0046872	< 0.0001
Cation binding	GO:0043169	< 0.0001
Organic cyclic compound binding	GO:0097159	< 0.0001

Table 3. List of genes that are expressed in fish exposed to both concentrations of PCB126 (3nM and 10nM). The expression levels (log FC) and statistical significance (False discovery rate) are shown.

		3 nM PCB126		10 nM PCB126	
Gene Description	**Gene Symbol**	**log FC**	**FDR**	**log FC**	**FDR**
Hairy-related 6	*her6*	1.32	2.67E-02	1.29	7.86E-03
Inhibin subunit beta Aa	*inhbaa*	-1.47	2.44E-02	-0.98	3.70E-02
Mitogen-activated protein kinase kinase kinase 15	*map3k15*	0.92	1.46E-02	1.46	2.09E-05
Solute carrier family 4 member 4a	*slc4a4a*	-1.07	2.67E-02	-1.14	4.43E-03
Guanylate cyclase 1 soluble subunit alpha 1	*gucy1a1*	1.25	4.71E-04	1.88	1.63E-06
frizzled class receptor 9b	*fzd9b*	1.53	4.54E-04	1.49	2.71E-04
si:ch211-195b13.1	*si:ch211-195b13.1*	1.59	1.86E-02	2.01	6.17E-04
Solute carrier family 3 member 1	*slc3a1*	-1.71	1.34E-03	-1.32	4.77E-03
Sulfotransferase family 1, cytosolic sulfotransferase 1	*sult1st1*	1.48	3.80E-02	2.09	6.68E-04
Feline leukemia virus subgroup C cellular receptor family, member 2a	*flvcr2a*	1.89	4.48E-02	2.26	3.40E-03
Complement component 1, q subcomponent binding protein	*c1qbp*	0.66	2.35E-02	0.68	4.36E-03
Integrin, beta-like 1	*itgbl1*	-1.38	1.58E-04	-1.74	2.40E-06
Cytochrome c oxidase subunit 6B1	*cox6b1*	1.13	2.67E-02	1.67	2.25E-04
Cytochrome P450, family 17, subfamily A, polypeptide 2	*cyp17a2*	-1.54	4.48E-02	-1.22	2.66E-02
Transmembrane protein 47	*tmem47*	1.04	2.67E-02	1.33	9.69E-04
Follistatin b	*fstb*	-2.17	2.53E-04	-2.68	7.51E-06
Leucine-rich repeat containing G protein-coupled receptor 4	*lgr4*	-0.91	4.44E-02	-0.67	3.83E-02
TCDD-inducible poly(ADP-ribose) polymerase	*tiparp*	0.68	2.67E-02	1.41	2.40E-06
Cytochrome P450, family 1, subfamily B, polypeptide 1	*cyp1b1*	4.61	1.98E-06	6.32	1.82E-08
si:ch211-197g15.7	*si:ch211-197g15.7*	1.09	2.35E-02	1.02	8.13E-03
Lymphatic vessel endothelial hyaluronic receptor 1a	*lyve1a*	-2.38	1.51E-02	-1.70	2.04E-02
FERM domain containing 4Bb	*frmd4bb*	1.09	1.67E-02	0.90	1.26E-02
N-acetyltransferase 8-like	*nat8l*	0.96	2.44E-02	1.22	8.08E-04
T cell immunoglobulin and mucin domain containing 4	*timd4*	3.91	1.39E-03	4.95	3.44E-05

Rho guanine nucleotide exchange factor (GEF) 19	*arhgef19*	1.29	2.88E-02	1.51	2.52E-03
CXXC finger protein 5a	*cxxc5a*	1.08	2.35E-02	1.99	7.51E-06
AL807829.1	*atp1a1b*	2.92	4.07E-02	2.85	1.08E-02
lipoprotein lipase	*lpl*	-1.32	4.56E-02	-1.06	2.62E-02
LincRNA	*FP017215.1*	3.07	2.53E-04	4.14	2.74E-06
Cytochrome P450, family 1, subfamily A	*cyp1a*	7.57	5.53E-10	8.96	6.55E-11
Cytochrome b5 type A (microsomal)	*cyb5a*	2.61	3.92E-04	4.28	8.78E-07
Muscle, skeletal, receptor tyrosine kinase	*musk*	2.56	1.40E-03	2.05	4.36E-03
Aryl-hydrocarbon receptor repressor a	*ahrra*	4.90	1.58E-04	6.31	2.74E-06
Cytochrome P450, family 1, subfamily C, polypeptide 1	*cyp1c1*	2.76	4.08E-03	4.22	2.09E-05

Table 4. Correlation between DNA methylation and gene expression. BAT_correlate function was used to determine the correlation. Mean methylation difference corresponds to the differentially methylated regions (DMRs) and log2 fold change corresponds to gene expression. *The location of DMR_70 on chromosome 5 in danRer10 version of the zebrafish genome converted to the exact location of DMR_34 in danRer7 version and therefore corresponds to the same gene. DMR_3 belongs to 3nM PCB126 group and the rest of them are from the 10nM PCB126 group.

DMR_ID	Gene ID	Gene Name	Mean Methylation Difference	Gene expression (log_2 fold change)	Spearman's Correlation (Adjusted p.value)
DMR_3	ENSDARG00000028661	Ciliary neurotrophic factor receptor (*cntfr*)	0.14	0.78	0.0279
DMR_10	ENSDARG00000015472	Glypican 4 (*gpc4*)	-0.23	1.16	0.0154
DMR_35	ENSDARG00000069311	Interleukin 15 receptor subunit alpha (*il15ra*)	-0.2	1.51	0.0022
DMR_34*	ENSDARG00000070845	si:dkey-56d12.4	-0.18	1.89	0.0022
DMR_70*	ENSDARG00000070845	si:dkey-56d12.4	-0.18	1.89	0.022
DMR_69	ENSDARG00000089382	zgc:158463	-0.2	1.21	0.0072
DMR_1	ENSDARG00000069996	DnaJ heat shock protein family (Hsp40) member B14 (*dnajb14*)	-0.4	0.9	0.0107
DMR_18	ENSDARG00000103318	Mitochondrial ribosomal protein L3 (*mrpl3*)	-0.47	0.41	0.0011
DMR_22	ENSDARG00000044718	Vav 2 guanine nucleotide exchange factor (*vav2*)	-0.20	-0.58	0.0046
DMR_30	ENSDARG00000013312	Ca^{++}- dependent secretion activator 2 (*cadps2*)	-0.20	-0.60	0.0004

Figure 1.

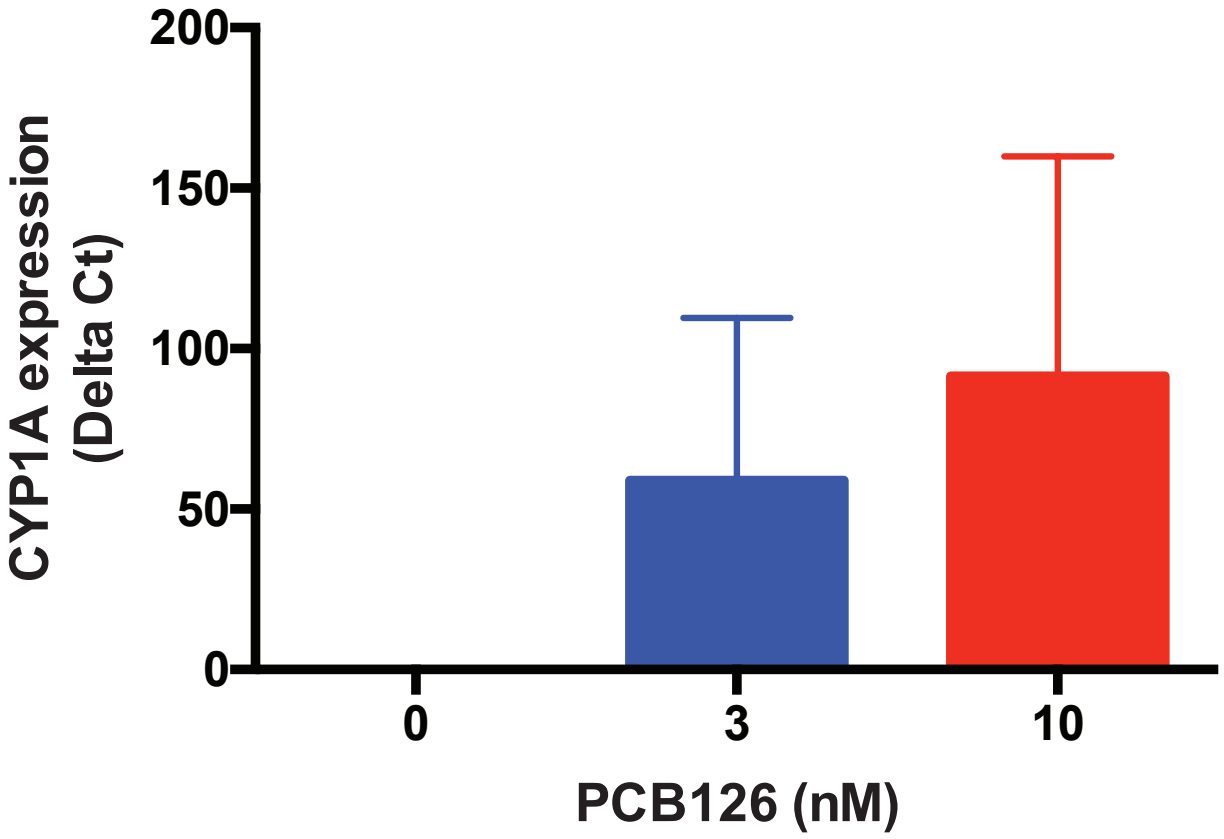

Figure 2.

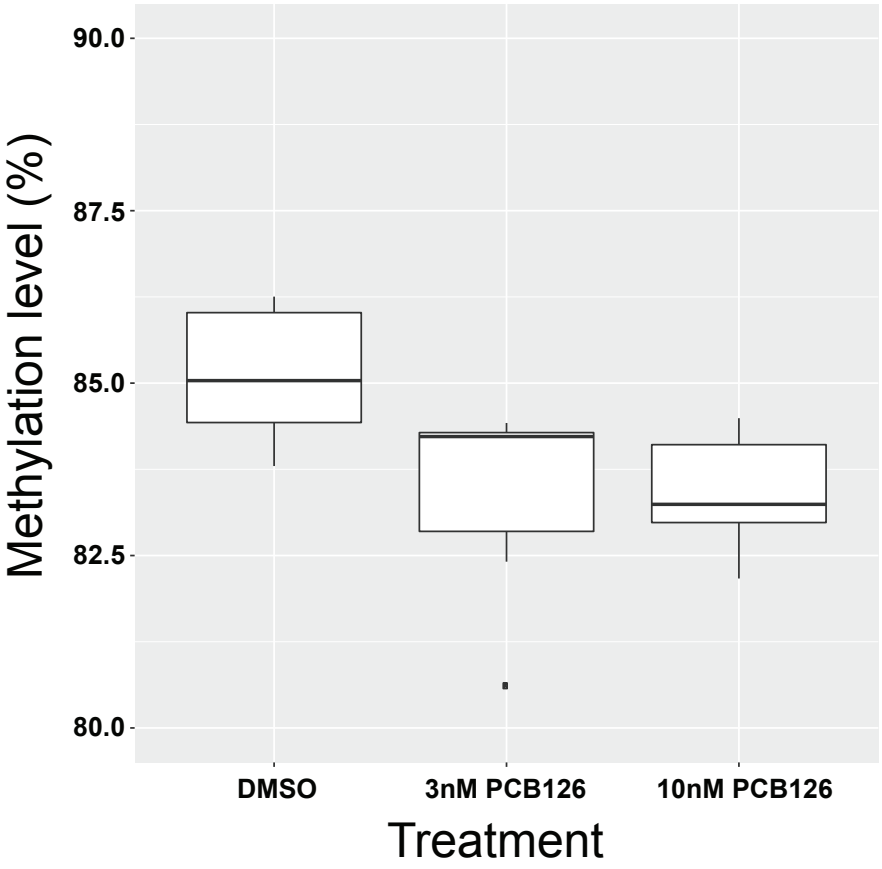
90.0
87.5
85.0
82.5
80.0
Methylation level (%)
DMSO
3nM PCB126
10nM PCB126
Treatment

Figure 3.

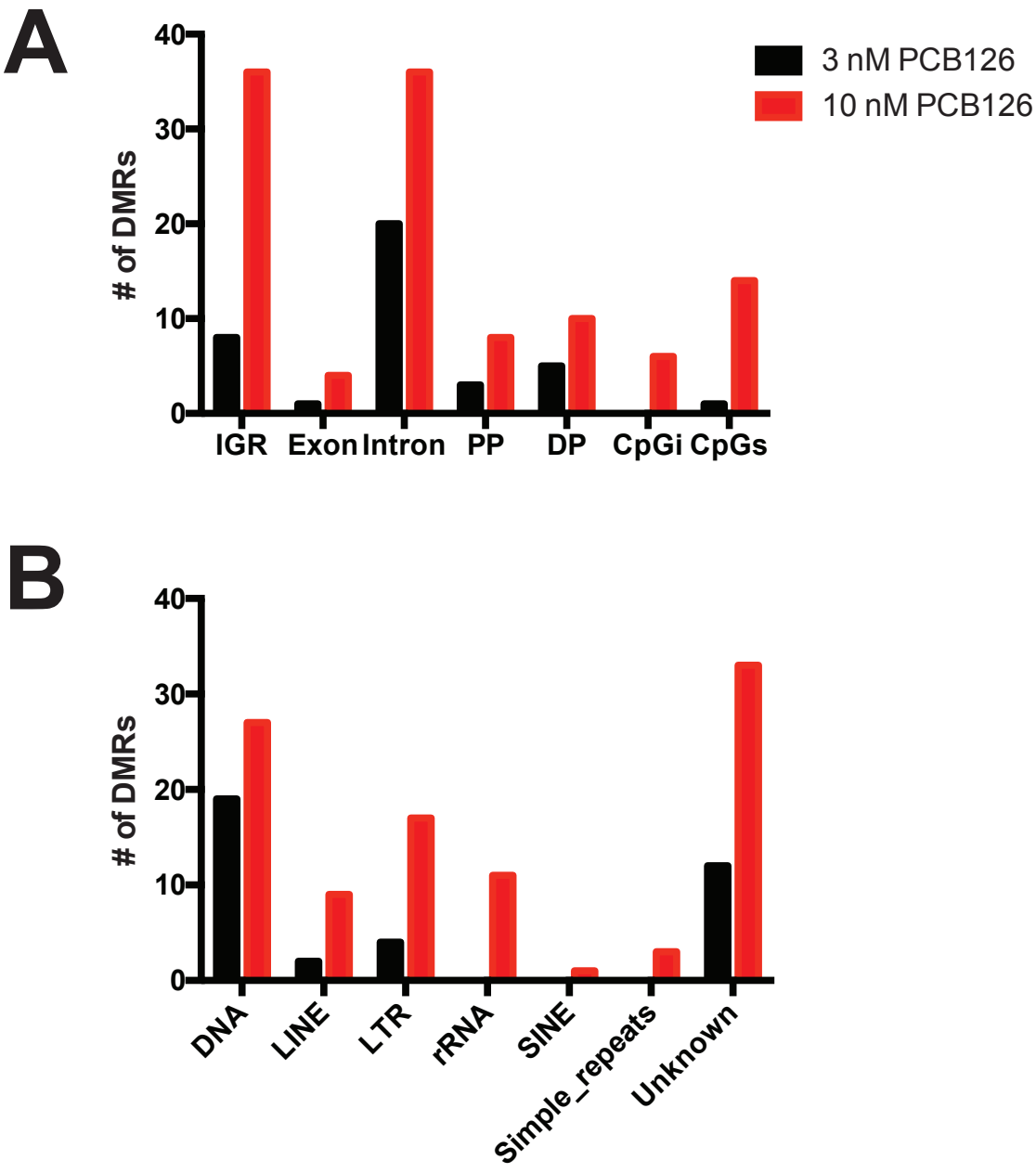
A
40
30
20
10
0
# of DMRs
3 nM PCB126
10 nM PCB126
IGR
Exon
Intron
PP
DP
CpGi
CpGs
B
40
30
20
10
0
# of DMRs
DNA
LINE
LTR
rRNA
SINE
Simple_repeats
Unknown

Figure 4.

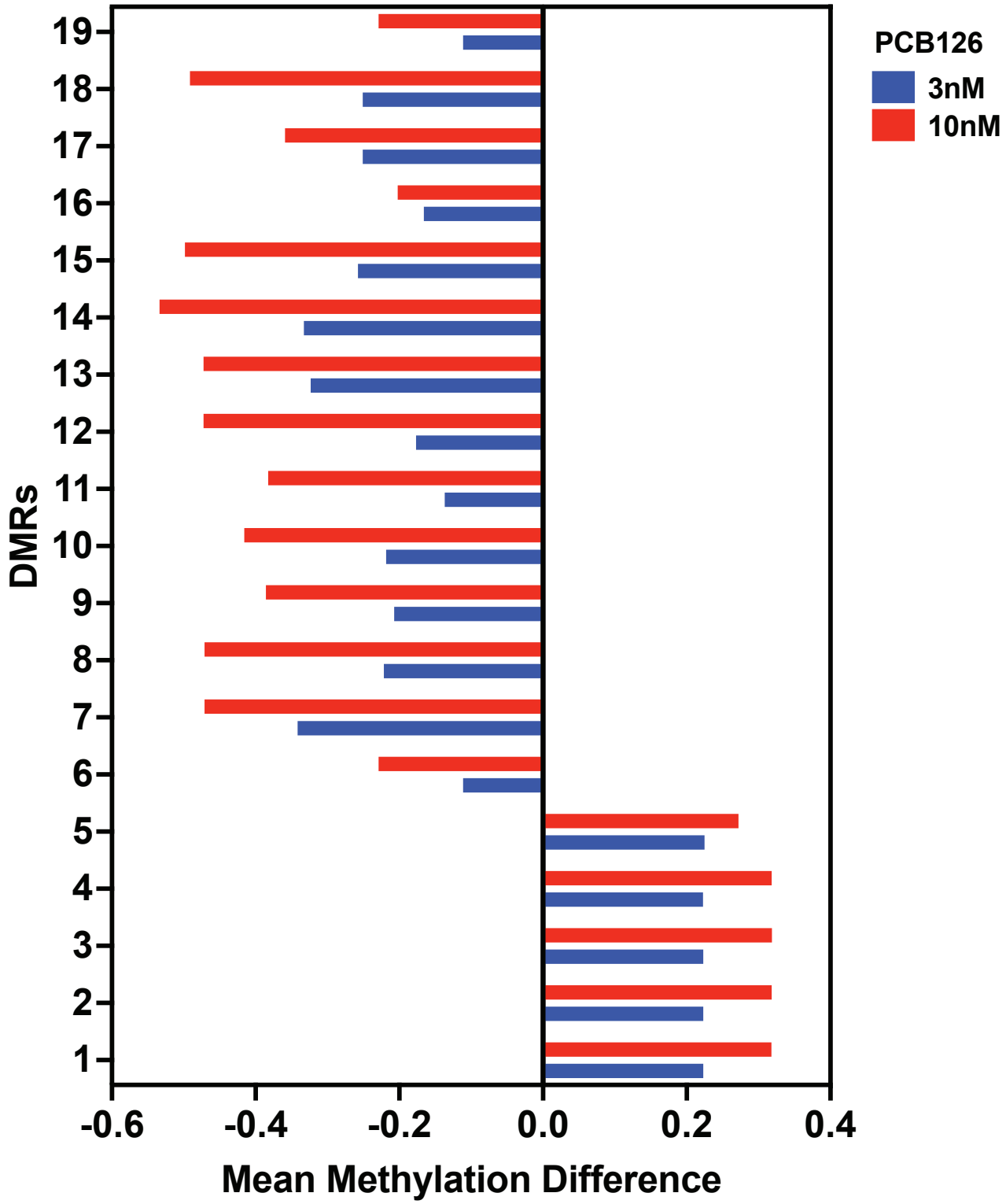
PCB126
3nM
10nM
DMRs
19
18
17
16
15
14
13
12
11
10
9
8
7
6
5
4
3
2
1
-0.6
-0.4
-0.2
0.0
0.2
0.4
Mean Methylation Difference

Figure 5.

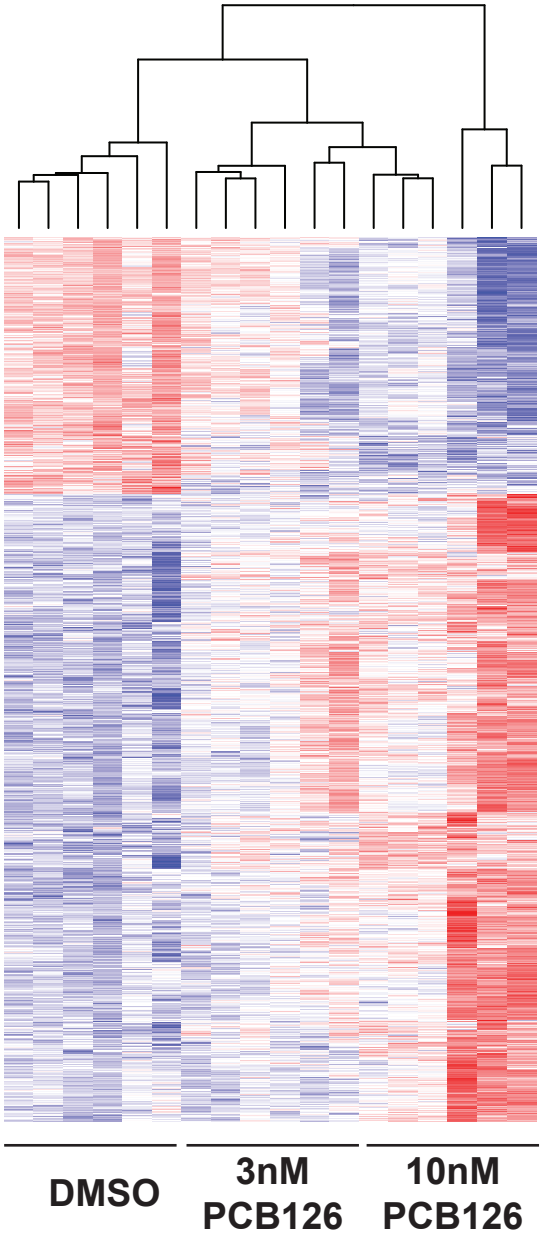

Figure 6.

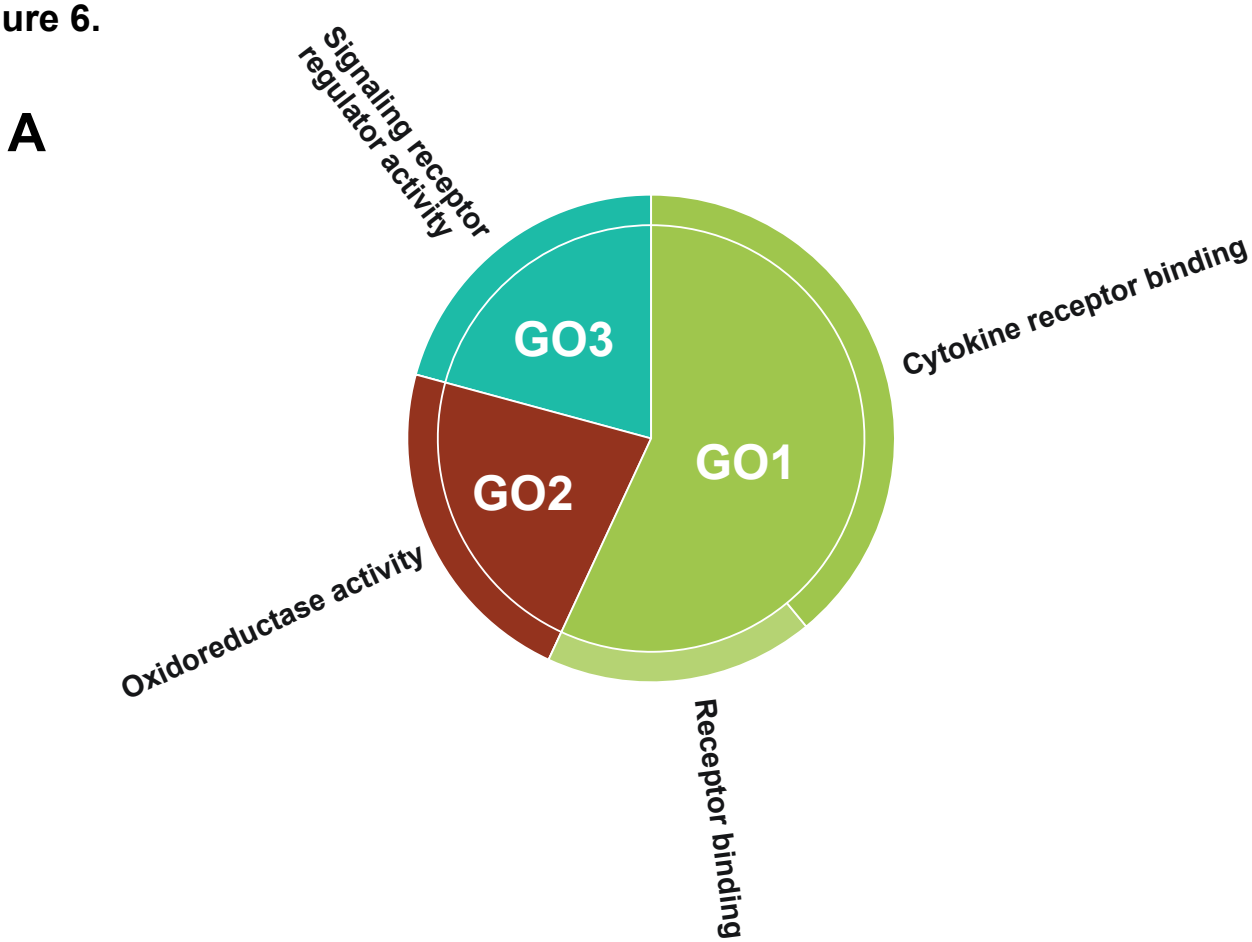
A
Signaling receptor regulator activity
Cytokine receptor binding
GO3
GO1
GO2
Oxidoreductase activity
Receptor binding

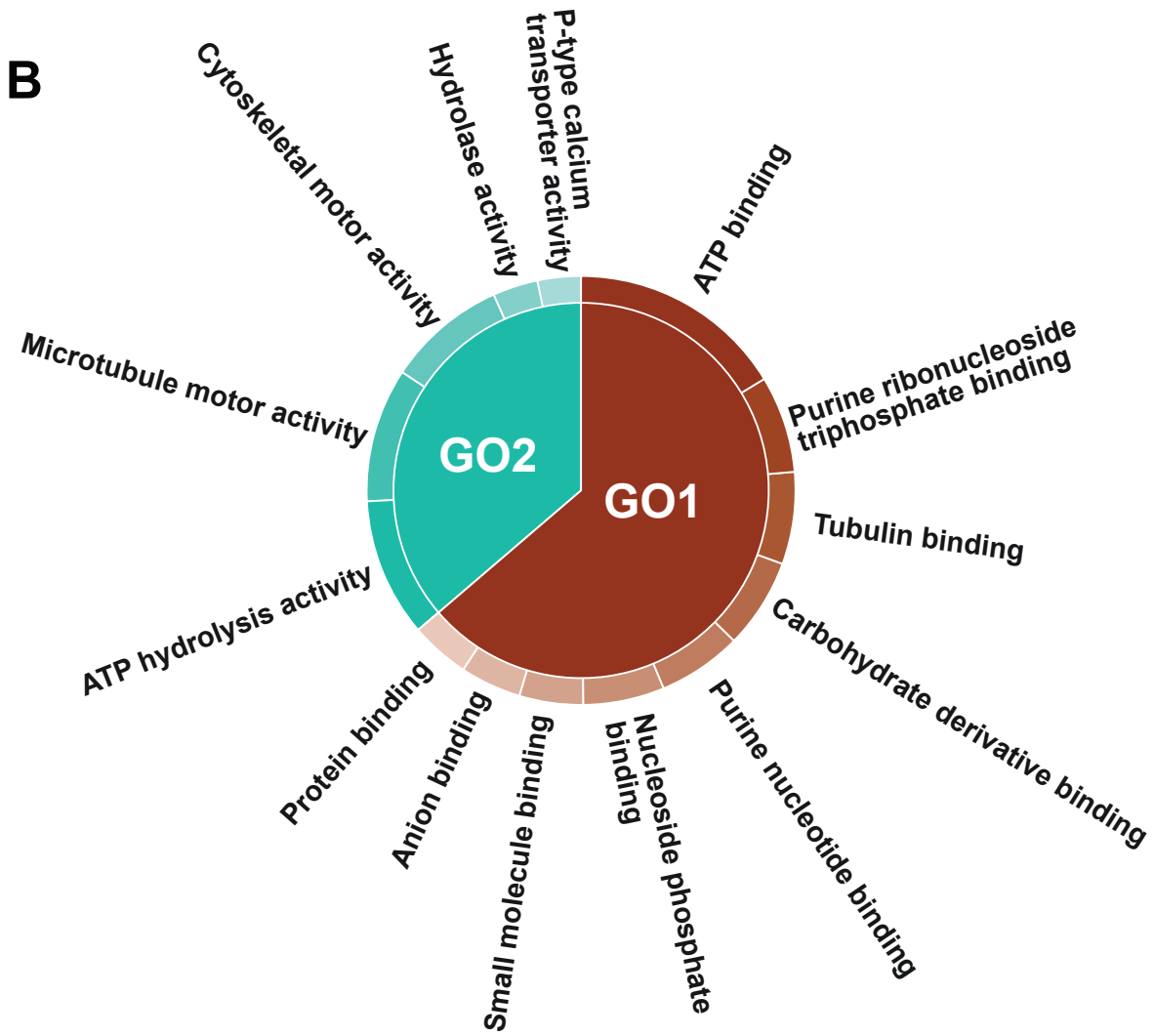
B
Cytoskeletal motor activity
Hydrolase activity
P-type calcium transporter activity
ATP binding
Microtubule motor activity
Purine ribonucleoside triphosphate binding
GO2
GO1
Tubulin binding
ATP hydrolysis activity
Carbohydrate derivative binding
Protein binding
Anion binding
Small molecule binding
Nucleoside phosphate binding
Purine nucleotide binding

Figure 7

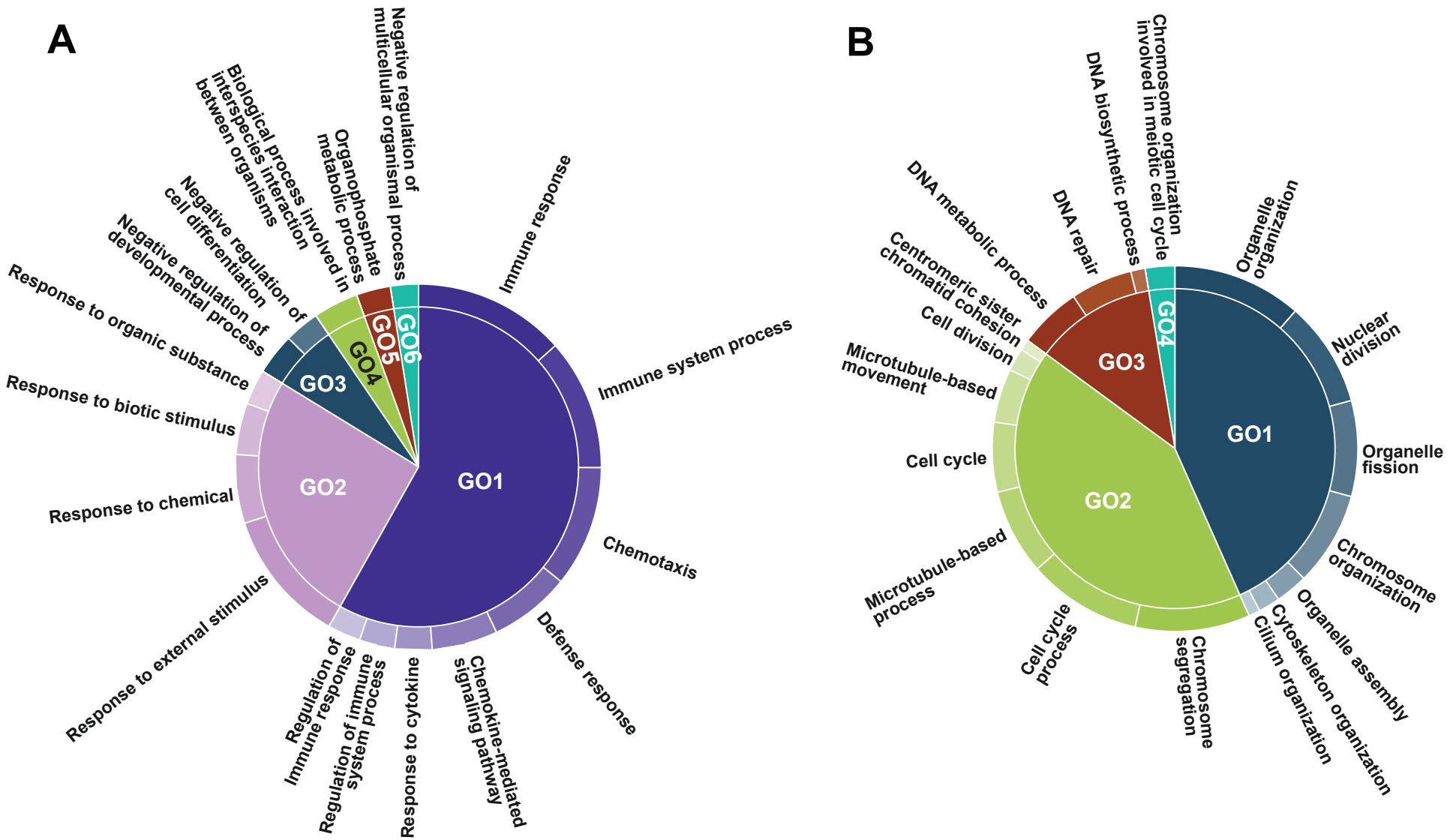
A
Negative regulation of multicellular organismal process
Biological process involved in interspecies interaction between organisms
Organophosphate metabolic process
Negative regulation of cell differentiation
Negative regulation of developmental process
Response to organic substance
Response to biotic stimulus
Response to chemical
Response to external stimulus
Regulation of Immune response
Regulation of immune system process
Response to cytokine
Chemokine-mediated signaling pathway
Defense response
Chemotaxis
Immune system process
Immune response
GO1
GO2
GO3
GO4
GO5
GO6
B
Chromosome organization involved in meiotic cell cycle
DNA biosynthetic process
DNA repair
DNA metabolic process
Centromeric sister chromatid cohesion
Cell division
Microtubule-based movement
Cell cycle
Microtubule-based process
Cell cycle process
Chromosome segregation
Cilium organization
Cytoskeleton organization
Organelle assembly
Chromosome organization
Organelle fission
Nuclear division
Organelle organization
GO1
GO2
GO3
GO4

Figure 8.

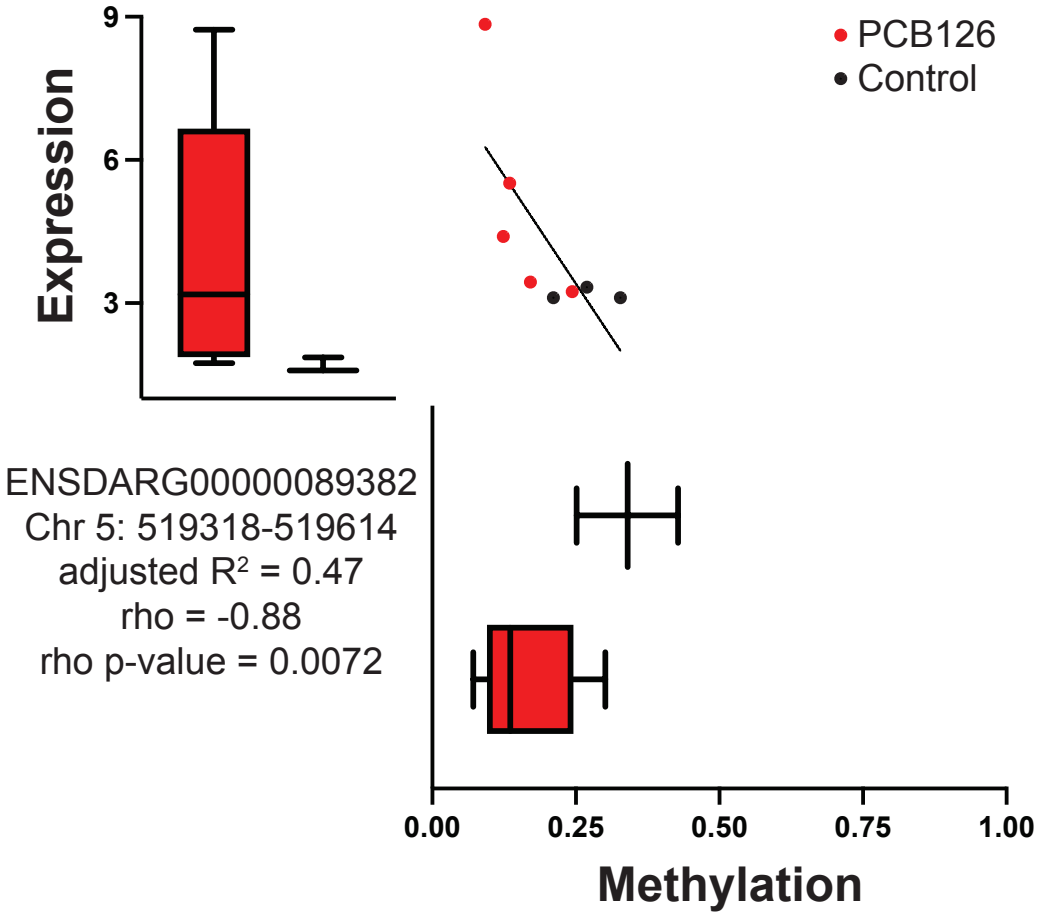
9
6
3
Expression
PCB126
Control
ENSDARG00000089382
Chr 5: 519318-519614
adjusted R² = 0.47
rho = -0.88
rho p-value = 0.0072
0.00
0.25
0.50
0.75
1.00
Methylation

Supplementary information

Exposure to 3, 3', 4, 4', 5-pentachlorobiphenyl (PCB 126) causes widespread DNA hypomethylation in adult zebrafish testis

Neelakanteswar Aluru[1] and Jan Engelhardt[2,3]

[1]Biology Department and Woods Hole Center for Oceans and Human Health, Woods Hole Oceanographic Institution, Woods Hole, MA 02543

[2]Bioinformatics Group, Department of Computer Science and Interdisciplinary Center for Bioinformatics, University of Leipzig, Härtelstraße 16-18, D-04107, Leipzig, Germany

[2]Department of Evolutionary Biology, University of Vienna, Djerassiplatz 1, A-1030 Vienna, Austria

Supplementary Table 1. Total number of raw and mapped reads from RRBS samples.

Condition	Sample ID	Number of reads	Number of mapped reads
DMSO	D1	8,168,404	7,632,045 (93.43%)
DMSO	D2	9,957,843	9,412,813 (94.53%)
DMSO	D3	10,786,595	10,233,729 (94.87%)
DMSO	D4	11,799,398	11,191,119 (94.84%)
DMSO	D5	14,501,290	13,578,935 (93.64%)
3nM PCB126	P3-9	13,635,225	12,757,987 (93.57%)
3nM PCB126	P3-11	13,674,864	12,977,478 (94.90%)
3nM PCB126	P3-12	11,830,503	11,269,978 (95.26%)
3nM PCB126	P3-13	13,968,933	13,279,248 (95.06%)
3nM PCB126	P3-14	12,536,363	11,890,055 (94.84%)
3nM PCB126	P3-16	12,210,513	11,558,361 (94.66%)
10nM PCB126	P10-17	11,824,432	11,224,550 (94.93%)
10nM PCB126	P10-18	9,949,807	9,424,059 (94.71%)
10nM PCB126	P10-21	10,983,355	10,403,421 (94.72%)
10nM PCB126	P10-23	12,880,370	12,242,973 (95.05%)
10nM PCB126	P10-24	11,786,444	11,224,951 (95.24%)
Average		**11,905,896**	**11,268,856 (94.65%)**

Supplementary Table 2. Total number of methylated and unmethylated reads in each sample.

Condition	Sample ID	Unmethylated CpGs (%)	Methylated CpGs (%)	Global methylation (%)
DMSO	D1	74,718 (5%)	1,430,201 (95%)	86%
DMSO	D2	103,721 (6%)	1,646,267 (94%)	85%
DMSO	D3	122,507 (7%)	1,733,399 (93%)	85%
DMSO	D4	144,119 (7%)	1,816,488 (93%)	84%
DMSO	D5	168,425 (7%)	2,096,685 (93%)	84%
3nM PCB126	P3-9	148,244 (7%)	1,979,684 (93%)	84%
3nM PCB126	P3-11	152,740 (7%)	1,983,935 (93%)	84%
3nM PCB126	P3-12	112,014 (6%)	1,769,691 (94%)	81%
3nM PCB126	P3-13	153,408 (7%)	1,999,865 (93%)	84%
3nM PCB126	P3-14	144,600 (7%)	1,923,376 (93%)	84%
3nM PCB126	P3-16	165,813 (8%)	1,797,084 (92%)	82%
10nM PCB126	P10-17	145,967 (8%)	1,757,976 (92%)	82%
10nM PCB126	P10-18	117,585 (7%)	1,681,977 (93%)	84%
10nM PCB126	P10-21	123,288 (6%)	1,805,228 (94%)	84%
10nM PCB126	P10-23	149,059 (7%)	1,882,976 (93%)	83%
10nM PCB126	P10-24	131,856 (7%)	1,764,152 (93%)	83%
Average		134,879 (7%)	1,816,810 (93%)	84%

Supplemental Figure 1. Hematoxylin and Eosin (H&E) staining of testicular tissue from different experimental groups. Representative images from control, 3nM and 10 nM PCB126-exposed groups are shown. Image J quantification did not reveal any significant differences in total area occupied by different testis cell types (spermatogonia, spermatids and spermatozoa).

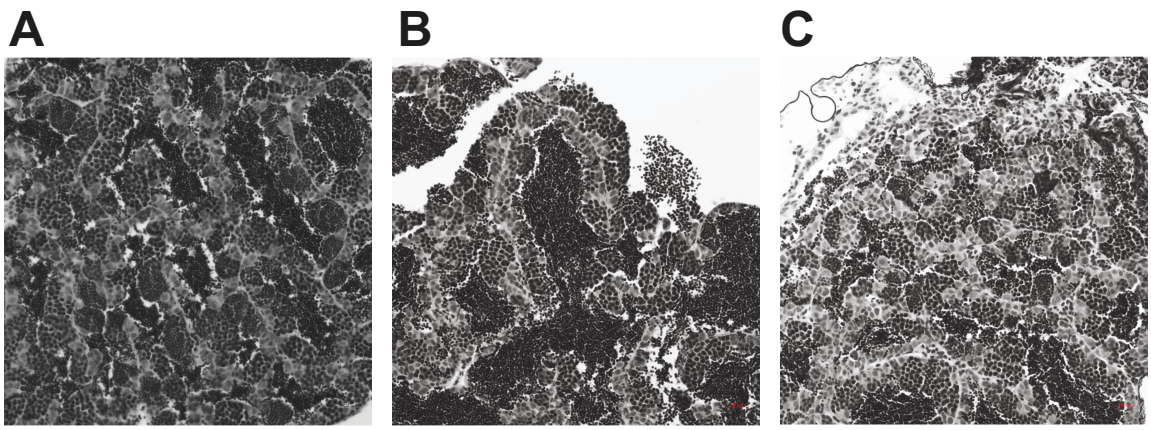

Supplemental Figure 2. Differentially methylated regions (DMRs) in response to PCB126 exposure. Volcano plots showing DMRs in response to 3nM PCB126 **(A)** and 10nM PCB126 **(B)** exposure. Percent methylation difference (x-axis) between PCB126 and Control are plotted against q-value (y-axis). Red vertical lines represent the methylation difference cutoff (15% for 3nM and 25% for 10nM PCB126) and the blue horizontal line represents a q-value of 0.05, which are used as a statistical cutoff in differential methylation analysis. Each green and red spot represents a statistically significant hypo and hypermethylated region, respectively.

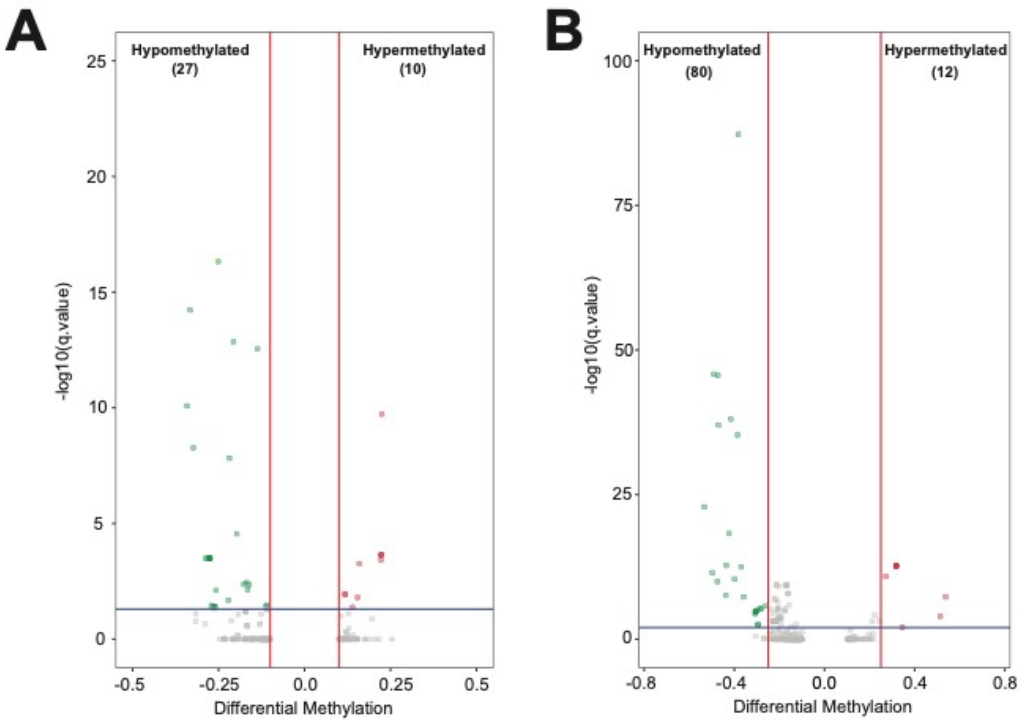

Instructions for visualizing the data RRBS and RNAseq data:

1. Go to UCSC genome browser home page (https://genome.ucsc.edu/).

2. Go to 'My Data'->'Track Hubs'->'My Hubs'

3. Paste " http://www.bioinf.uni-leipzig.de/~jane/Neel/testisRRBSHub/hub.txt" into the URL window and click "Add Hub". This will load the data.

4. Click on the hyperlink danRer10 to view the data.

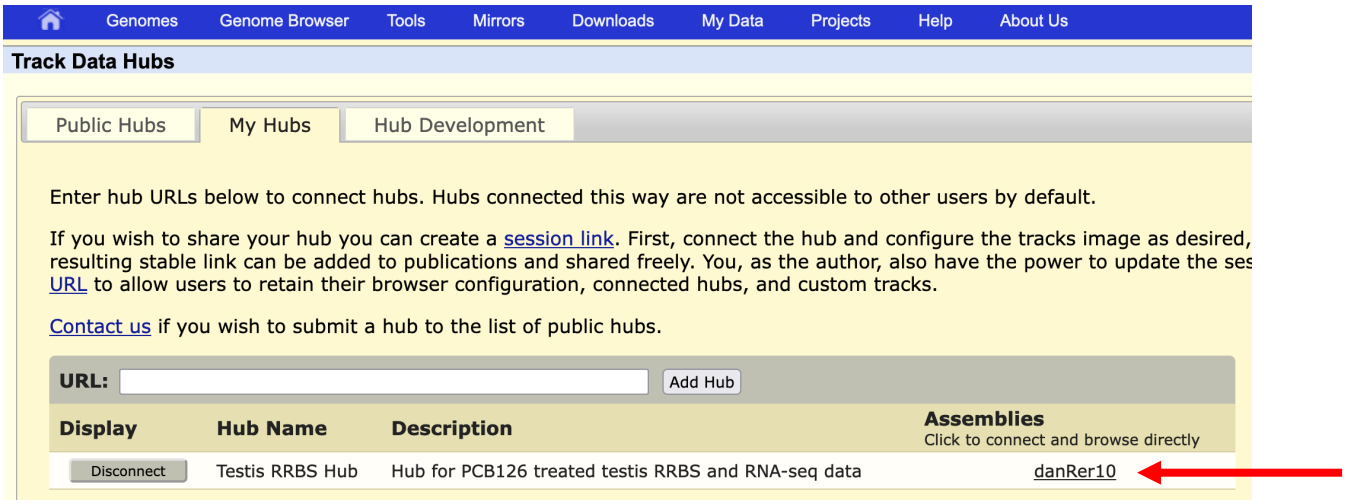

5. Screenshot of the data

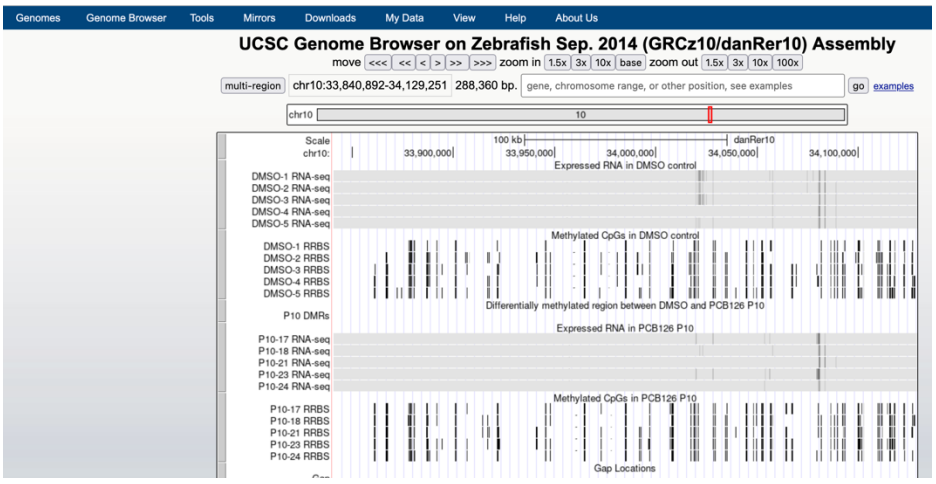

6. Type a DMR coordinates (e.g., chr4:30,435,323-30,435,952) or browse through the entire data by each chromosome.